

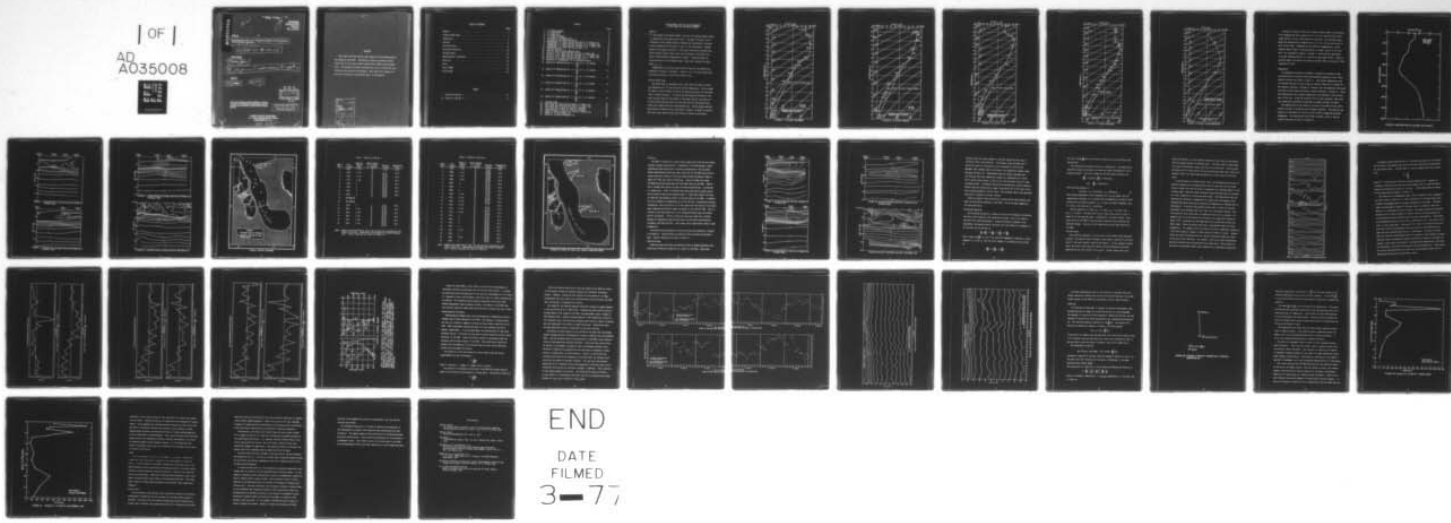
AD-A035 008 NAVAL OCEANOGRAPHIC OFFICE WASHINGTON D C MARINE SC--ETC F/G 8/10
A PRELIMINARY STUDY OF THE OCEANOGRAPHY OF THE TONGUE OF THE OC--ETC(U)
JUN 62 E L RIDLEY

UNCLASSIFIED

N00-IM-0-39-62

NL

| OF |
AD
A035008



END
DATE
FILMED
3-77

461a

ADA035008

MOST Project - 2

INFORMAL
MANUSCRIPT
REPORT
NO. 0-39-62

Good

1 DD

TITLE

6

A PRELIMINARY STUDY OF THE OCEANOGRAPHY OF THE TONGUE
OF THE OCEAN, BAHAMAS.

14

NOCR-IM-0-39-62

AUTHOR

10

EDWARD L. RIDLEY

9

Informal manuscript rept.,

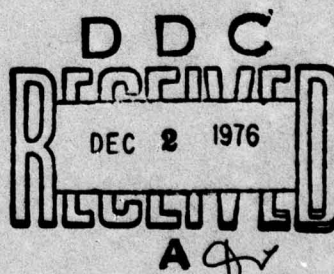
DATE

11

JUN 1962

12

45 p.



This manuscript has a limited distribution, therefore
in citing it in a bibliography, the reference should be
followed by the phrase UNPUBLISHED MANU-
SCRIPT.

DISTRIBUTION STATEMENT A

Approved for public release;
Distribution Unlimited

MARINE SCIENCES DEPARTMENT
U. S. NAVAL OCEANOGRAPHIC OFFICE
WASHINGTON 25, D.C.

401 263 ✓

mt

ABSTRACT

This report outlines briefly some aspects of the oceanography of the Tongue of the Ocean. Variations in physical properties occur within two or three hours which significantly affect sound propagation. The observed variations preclude the use of conventional data collection and processing techniques. More definitive reports will follow as warranted by significant gains in information.

ACCESSION for	
RTIS	White Section <input checked="" type="checkbox"/>
DOC	Buff Section <input type="checkbox"/>
UNANNOUNCED	<input type="checkbox"/>
JUSTIFICATION	<i>Letter on file</i>
BY	
DISTRIBUTION/AVAILABILITY CODES	
DISP.	AVAIL. REG. & SPECIAL
A	

TABLE OF CONTENTS

	Page
General	1
Surface Mixed Layer	1
Temperature	7
Salinity	15
Time Variations	15
Horizontal Advection	18
Internal Waves	19
Meteorological Influences	27
Stability	32
Tides	37
Future Study	37
Bibliography	40

TABLES

I. Results of Run No. 1	12
II. Results of Run No. 2	13

FIGURES

	Page
1. T-S CURVE-DECEMBER	2
2. T-S CURVE-MARCH	3
3. T-S CURVE-JULY	4
4. T-S CURVE-SEPTEMBER	5
5. T-S CURVE-30 SEPTEMBER 1958	6
6. DISTRIBUTION OF OXYGEN WITH DEPTH	8
7. TEMPERATURE ($^{\circ}$ C) CROSS SECTION STATIONS 3-6 16 MARCH 1960	9
8. TEMPERATURE ($^{\circ}$ C) CROSS SECTION STATIONS 10-12 18 MARCH 1960	9
9. TEMPERATURE ($^{\circ}$ C) CROSS SECTION STATIONS 15-18 19 MARCH 1960	10
10. TEMPERATURE ($^{\circ}$ C) CROSS SECTION STATIONS 1-18	10
11. STATION LOCATIONS	11
12. TRACK OF SHALLOW WATER SAMPLING RUNS	14
13. SALINITY ($^{0}/oo$) CROSS SECTION STATIONS 3-6 MARCH 1960	16
14. SALINITY ($^{0}/oo$) CROSS SECTION STATIONS 10-12 18 MARCH 1960	16
15. SALINITY ($^{0}/oo$) CROSS SECTION STATIONS 15-18 19 MARCH 1960	17
16. SALINITY ($^{0}/oo$) CROSS SECTION STATIONS 1-18	17
17. VARIATION IN TEMPERATURE ($^{\circ}$ C) AT INDICATED DEPTHS	21
18. RESULTS OF COMPUTATIONS OF $\eta = \frac{T^1}{dT} \text{ AT } Z = 150 \text{ METERS}$	23
19. RESULTS OF COMPUTATIONS OF $\eta = \frac{T^1}{dT} \text{ AT } Z = 225 \text{ METERS}$	23
20. RESULTS OF COMPUTATIONS OF $\eta = \frac{T^1}{dT} \text{ AT } Z = 250 \text{ METERS}$	24
21. RESULTS OF COMPUTATIONS OF $\eta = \frac{T^1}{dT} \text{ AT } Z = 650 \text{ METERS}$	24
22. RESULTS OF COMPUTATIONS OF $\eta = \frac{T^1}{dT} \text{ AT } Z = 700 \text{ METERS}$	25
23. RESULTS OF COMPUTATIONS OF $\eta = \frac{T^1}{dT} \text{ AT } Z = 750 \text{ METERS}$	25
24. INTERNAL WAVES	26
25. WIND SPEED AND DIRECTION-SAN PABLO-9-16 MARCH 1962	29
26. WIND SPEED AND DIRECTION-SAN PABLO-17-22 MARCH 1962	29
27. TIME VARIATION IN DEPTH OF SELECTED ISOTHERMS	30
28. TIME VARIATION IN DEPTH OF SELECTED ISOTHERMS	31
29. CHANGE IN DENSITY CAUSED BY A VERTICAL MIGRATION dZ	33
30. STABILITY VS DEPTH-MARCH 1962	35
31. STABILITY VS DEPTH-SEPTEMBER 1961	36

A PRELIMINARY STUDY OF THE OCEANOGRAPHY OF THE TONGUE OF THE OCEAN, BAHAMAS

General

→ The Tongue of the Ocean (TOTO), like the surrounding oceanic waters, is composed of three major water types. The upper 250 meters are influenced by local meteorological processes and the physical structure varies seasonally and from year to year in the same season. Between depths of 250 meters and 800 to 1,000 meters the waters are basically North Atlantic Central Water, and near the bottom a relatively thin layer of North Atlantic Deep Water is found. Transition zones of varying mixtures of two adjacent water types occur between the major types. ←

Temperature vs salinity curves (T-S) for each of the seasons are presented in Figures 1 through 4. Figure 5 is a T-S curve constructed from data collected in the Florida Straits area.

Surface Mixed Layer

The mixed layer is defined as that layer above the depth at which the temperature is 1°C less than the surface temperature. During summer off Andros Island at about $24^{\circ} 45' \text{N}$, the maximum thickness of the mixed layer is about 70 meters. In the spring the maximum thickness of this layer may be as much as 200 meters in the same locality, but data collected during different years for the same locality and seasons show mixed layer depths which are considerably less. During autumn the maximum observed thickness varies from about 55 meters to about 115 meters. The mixed layer depth during winter may be as great as 225 meters.

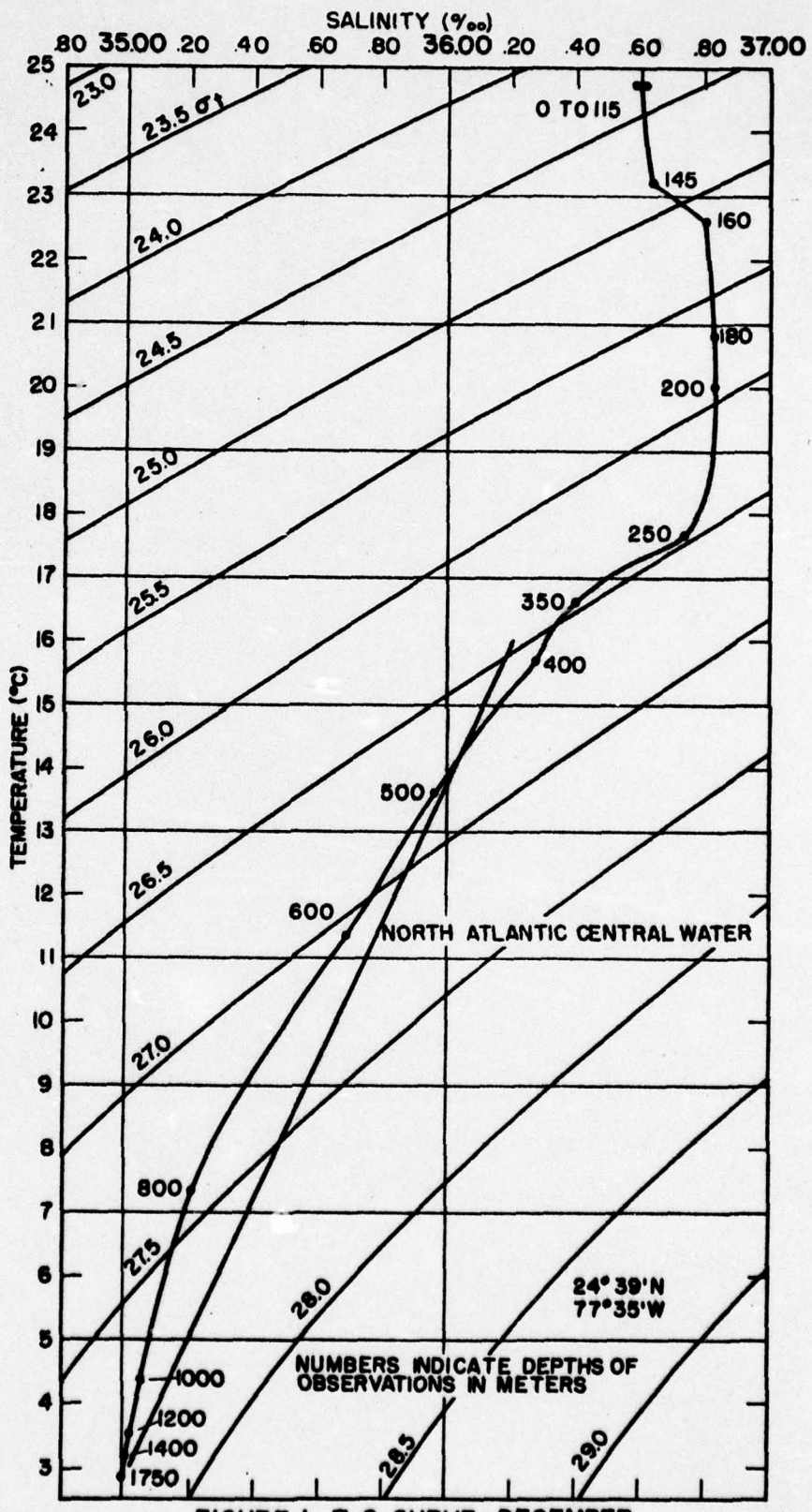


FIGURE 1 T-S CURVE - DECEMBER

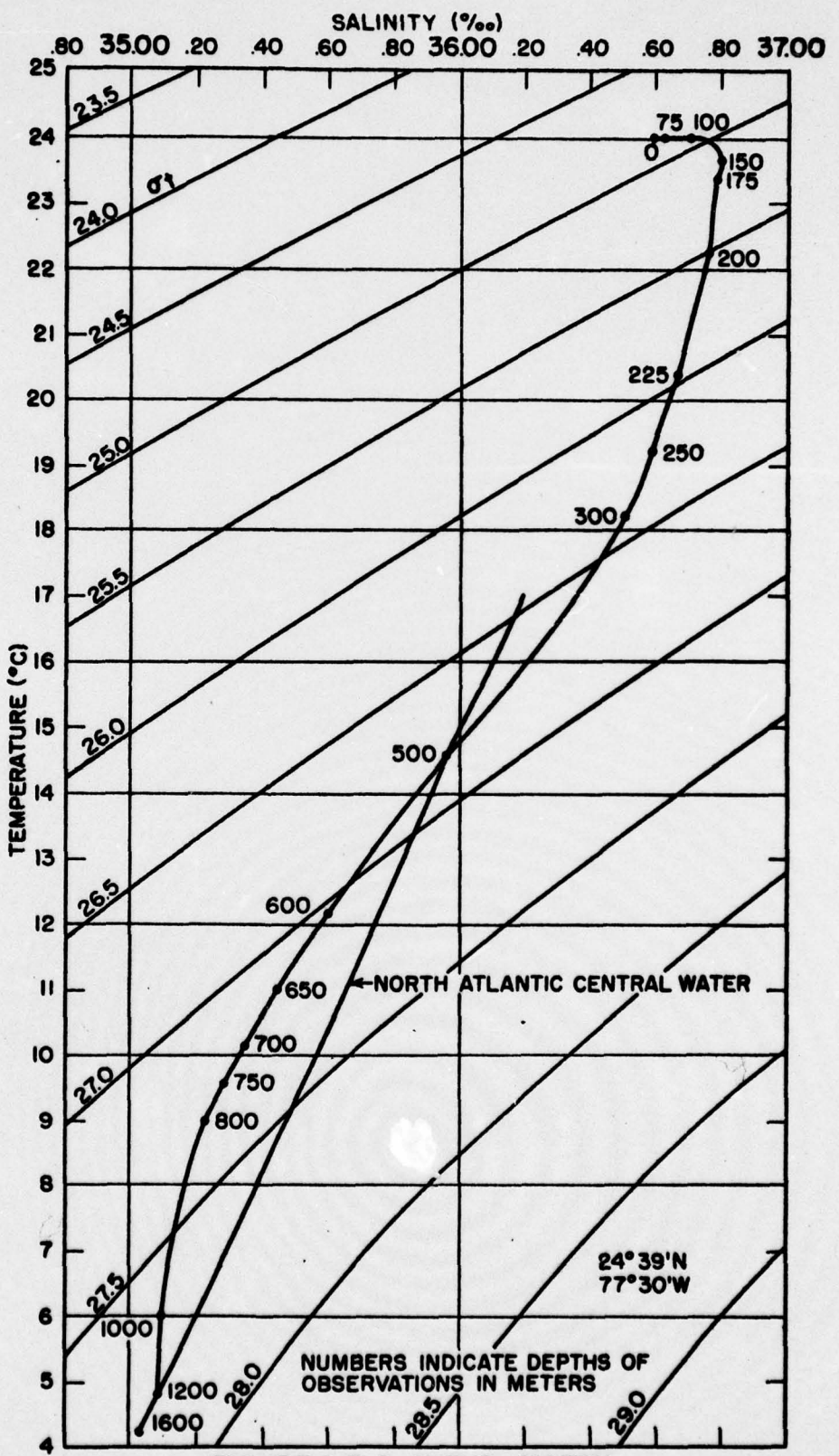
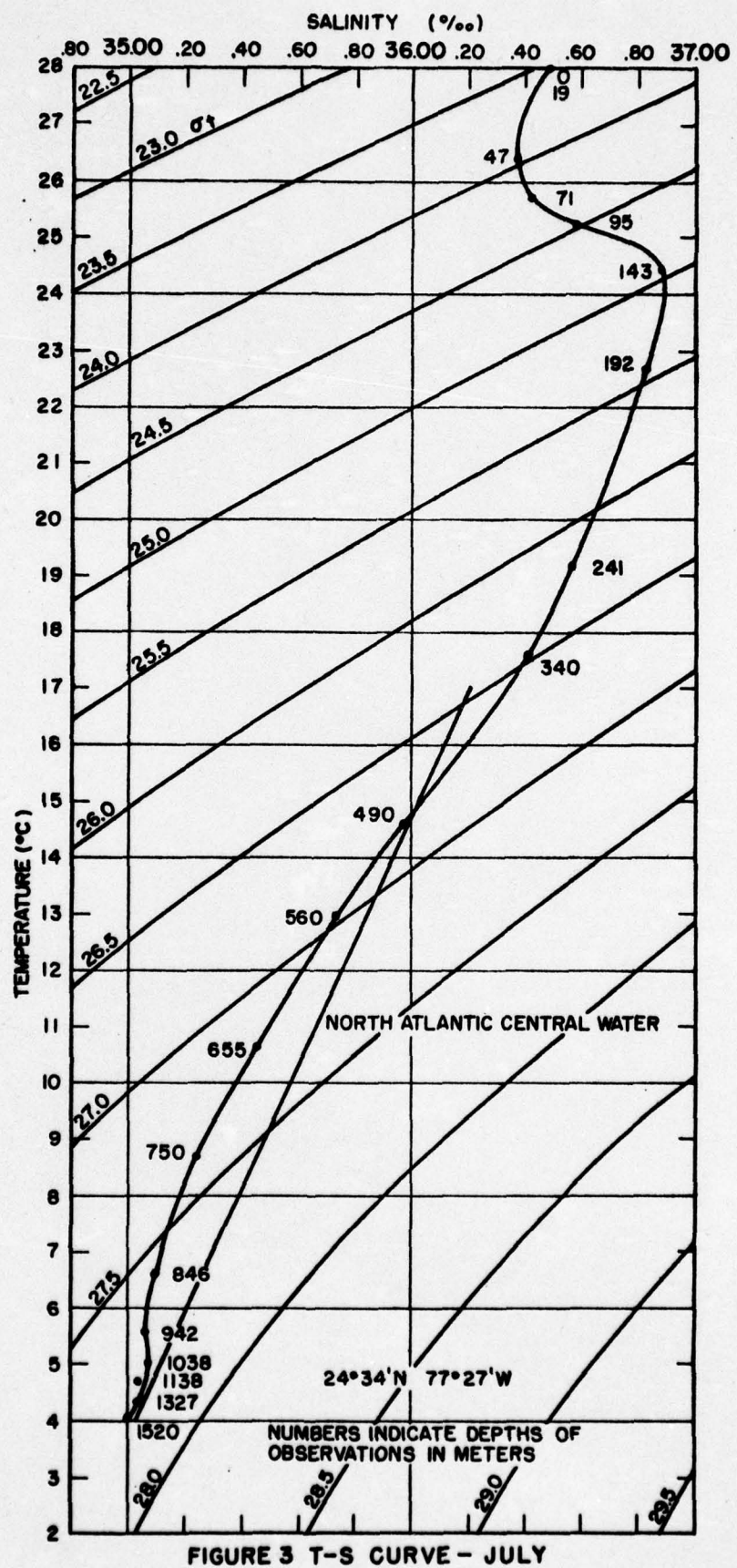


FIGURE 2 T-S CURVE - MARCH



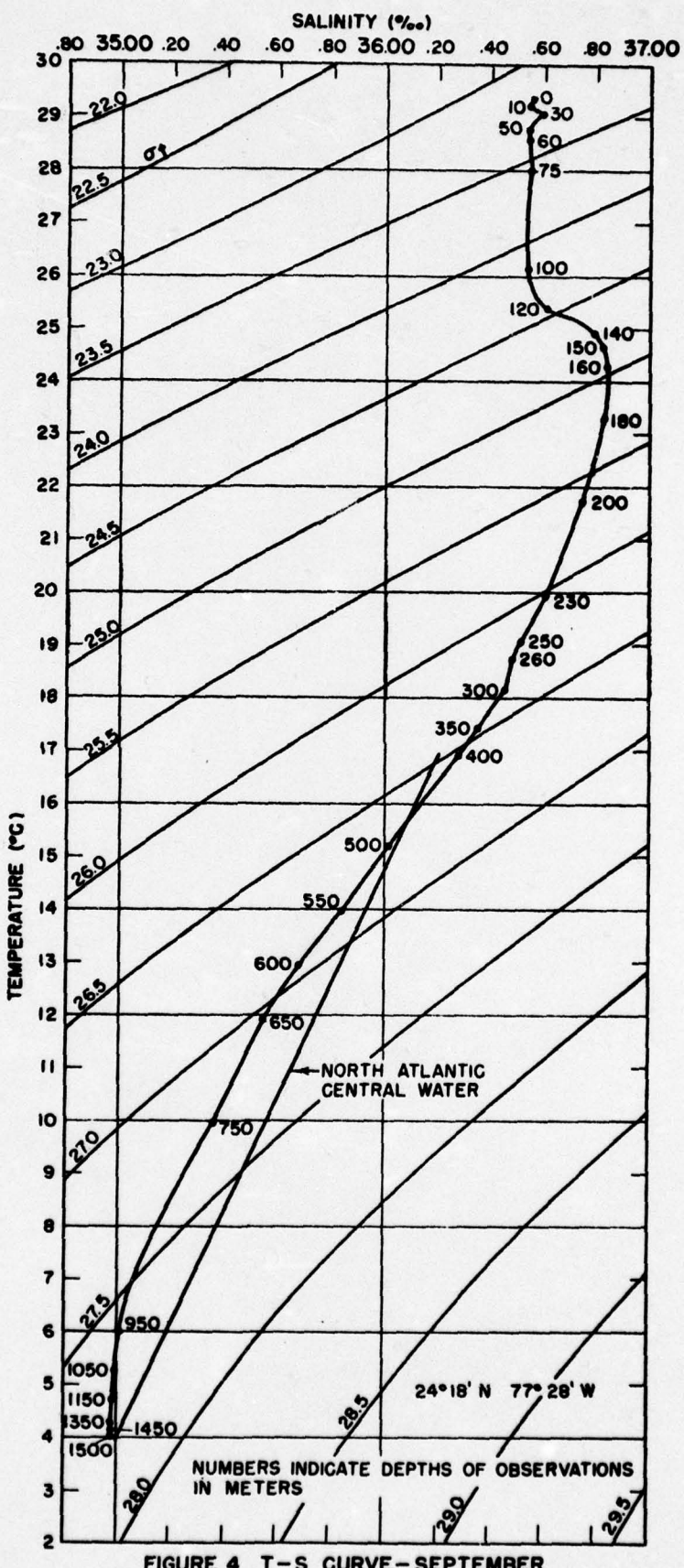


FIGURE 4 T-S CURVE - SEPTEMBER

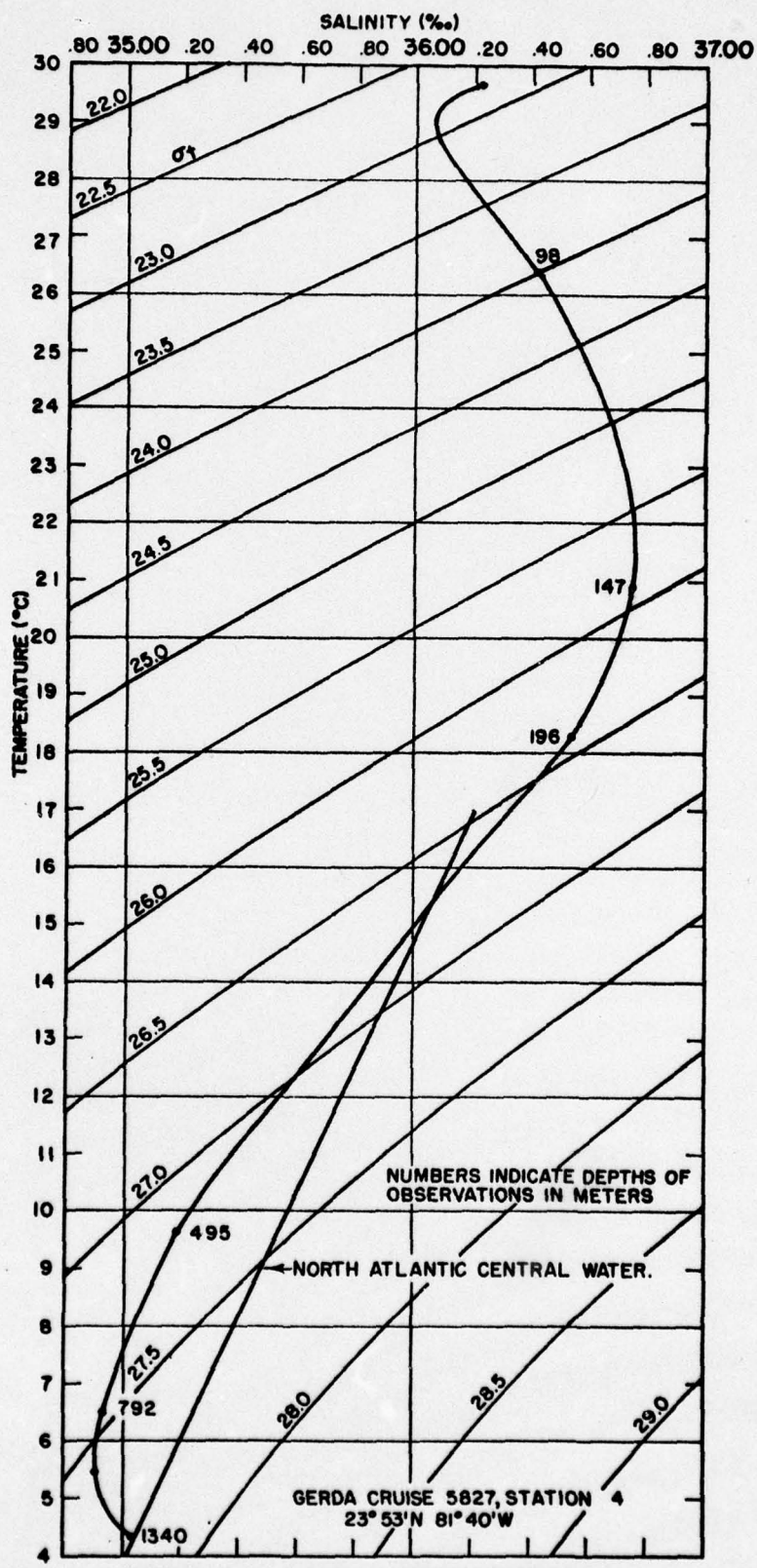


FIGURE 5 T-S CURVE - 30 SEPTEMBER 1958

According to Defant (1960) North Atlantic Central Water has characteristic temperatures which range from 4.0° to 17.0°C and salinities which range from 35.1 to 36.2 ‰ (parts per thousand). North Atlantic Deep Water has characteristic temperatures of 3.0° to 4.0°C and salinities of 34.8 to 34.9 ‰. (Temperatures are potential temperatures.) North Atlantic Central Water is represented by a straight line on a T-S curve and is so indicated on Figures 1 through 5. North Atlantic Deep Water is further characterized by its relatively high oxygen content. Figure 6 presents depth distribution of oxygen during May 1958 at latitude 23° 58'N, longitude 77° 19'W.

Temperature

The temperature profiles of Figures 7 through 10 are based on data collected from 4 to 20 March 1960 and previously presented in H.O. TR-94. Station locations are shown in Figure 11. The surface temperatures show an increase from west to east along the northern (Stations 15 through 18) and southern (Stations 3 through 6) transects, but the temperature decreases from west to east along the central transect (Stations 3 through 6). Along the longitudinal axis, highest temperatures were observed in the northern part of the area. Along the verticals at all three transects, small positive temperature gradients existed down to depths of about 150 meters.

The temperatures of the shoals to the east of the TOTO are not sufficiently accurate to establish any horizontal gradients. The range of temperature is from about 77°F (25°C) to 79°F (26°C) as measured by bucket thermometer. The observations are listed in Tables I and II, and the station locations are shown in Figure 12.

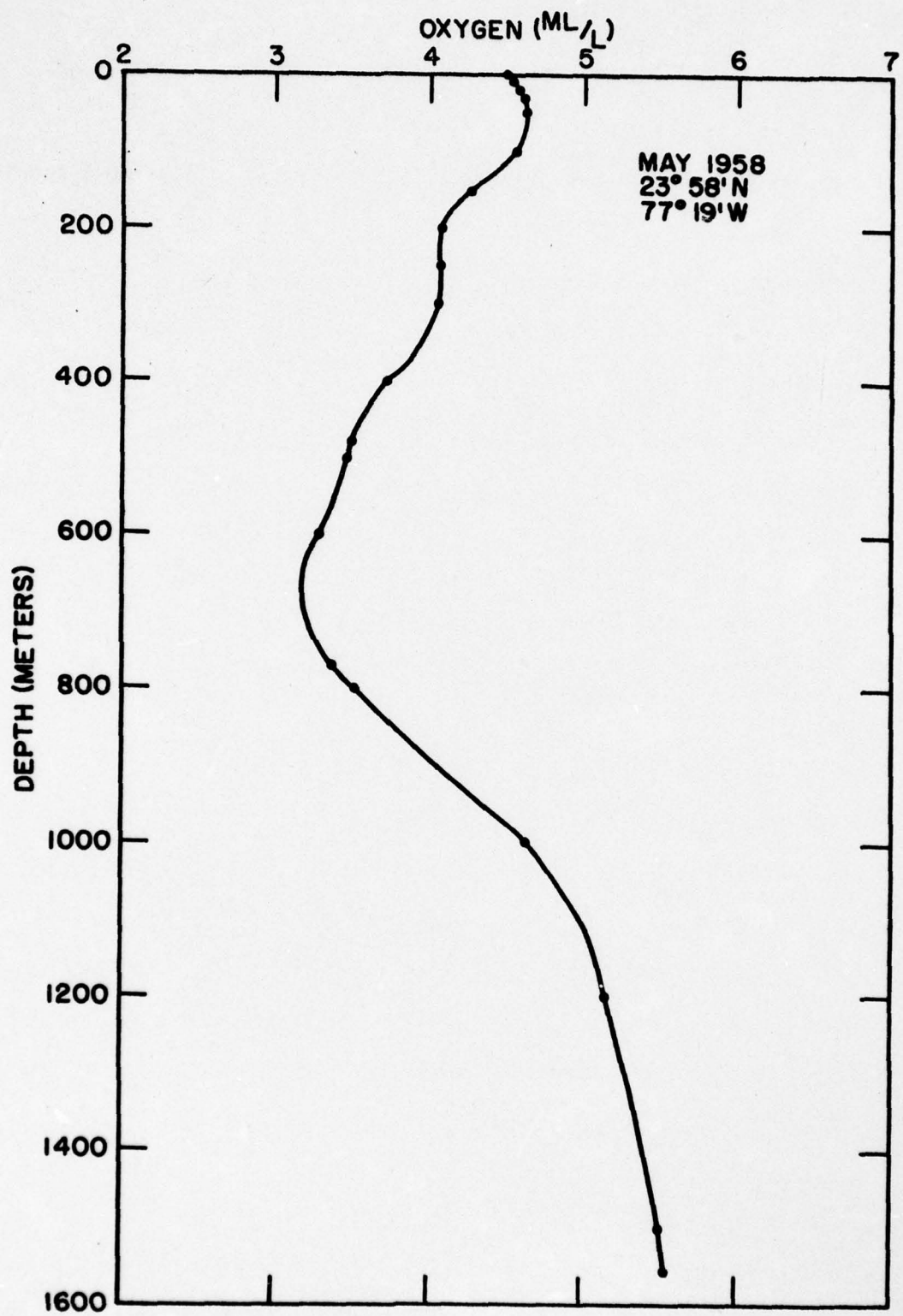
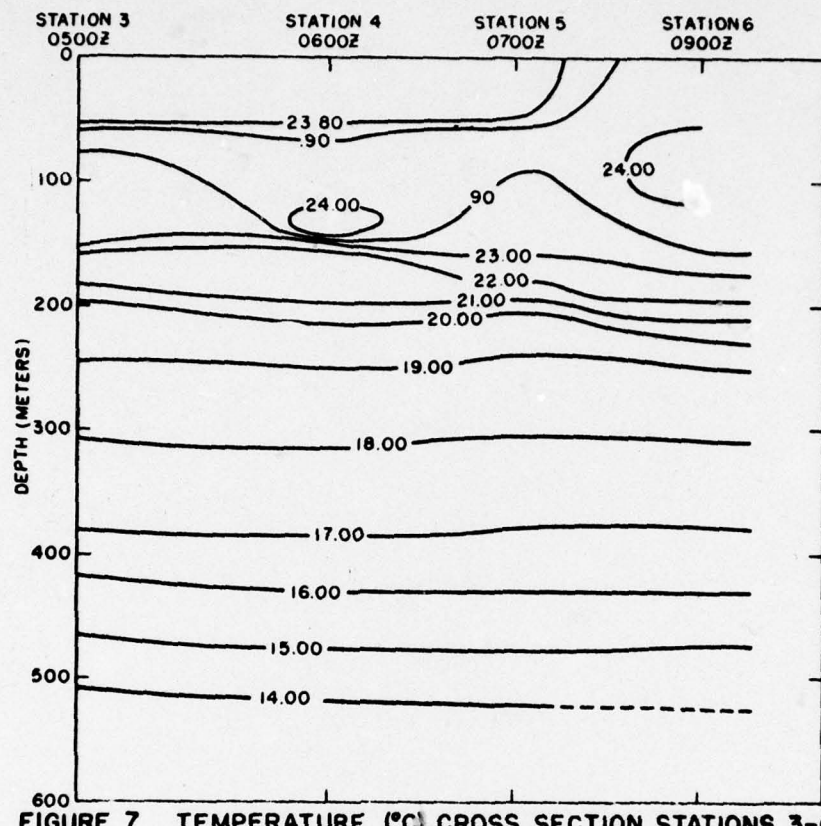
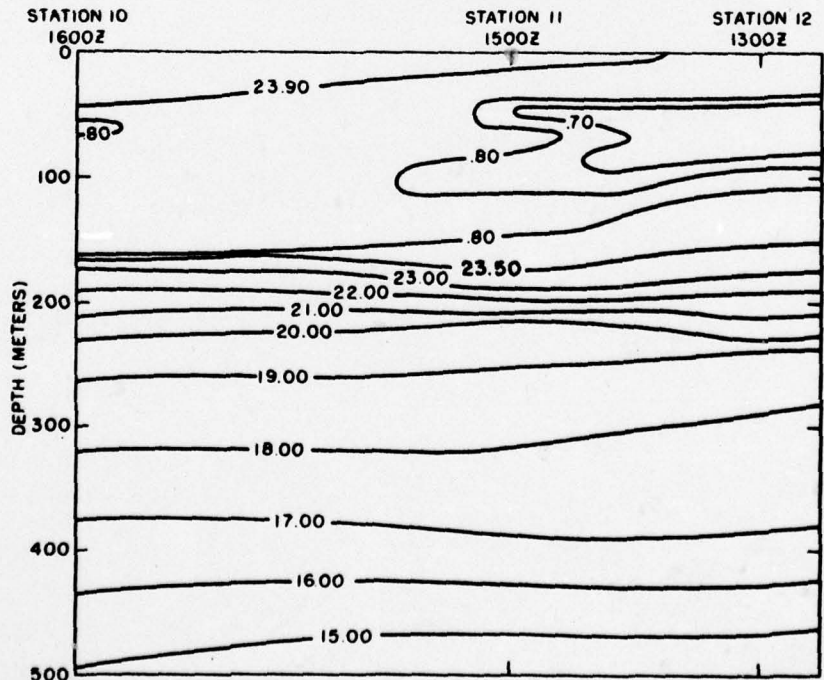


FIGURE 6 DISTRIBUTION OF OXYGEN WITH DEPTH



**FIGURE 7 TEMPERATURE (°C) CROSS SECTION STATIONS 3-6
16 MARCH 1960**



**FIGURE 8 TEMPERATURE (°C) CROSS SECTION STATIONS 10-12
18 MARCH 1960**

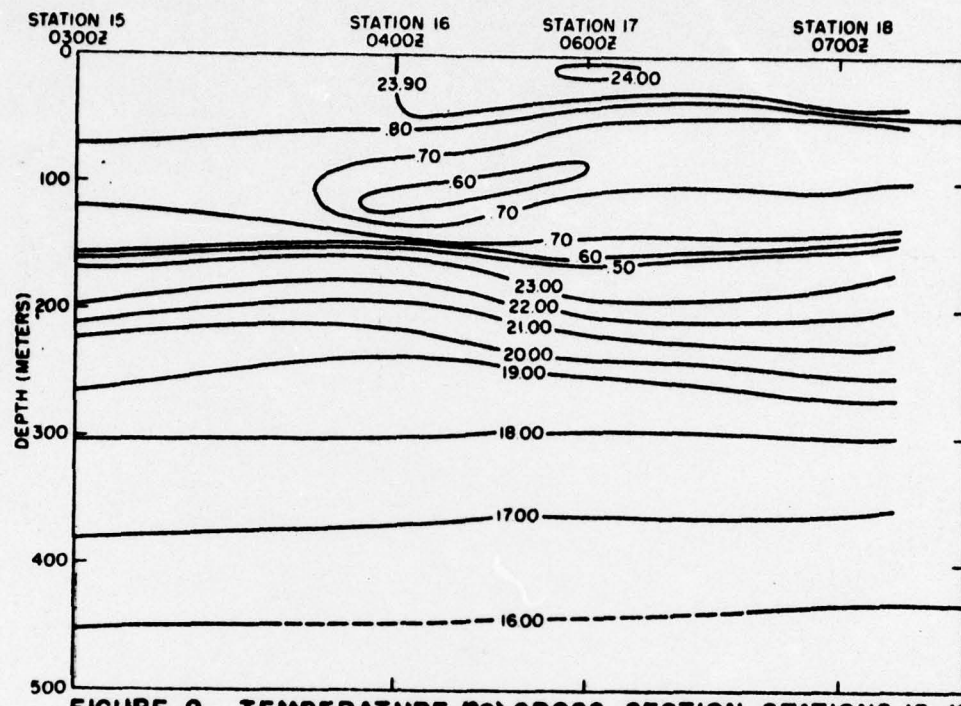


**FIGURE 9 TEMPERATURE (°C) CROSS SECTION STATIONS 15-18
19 MARCH 1960**

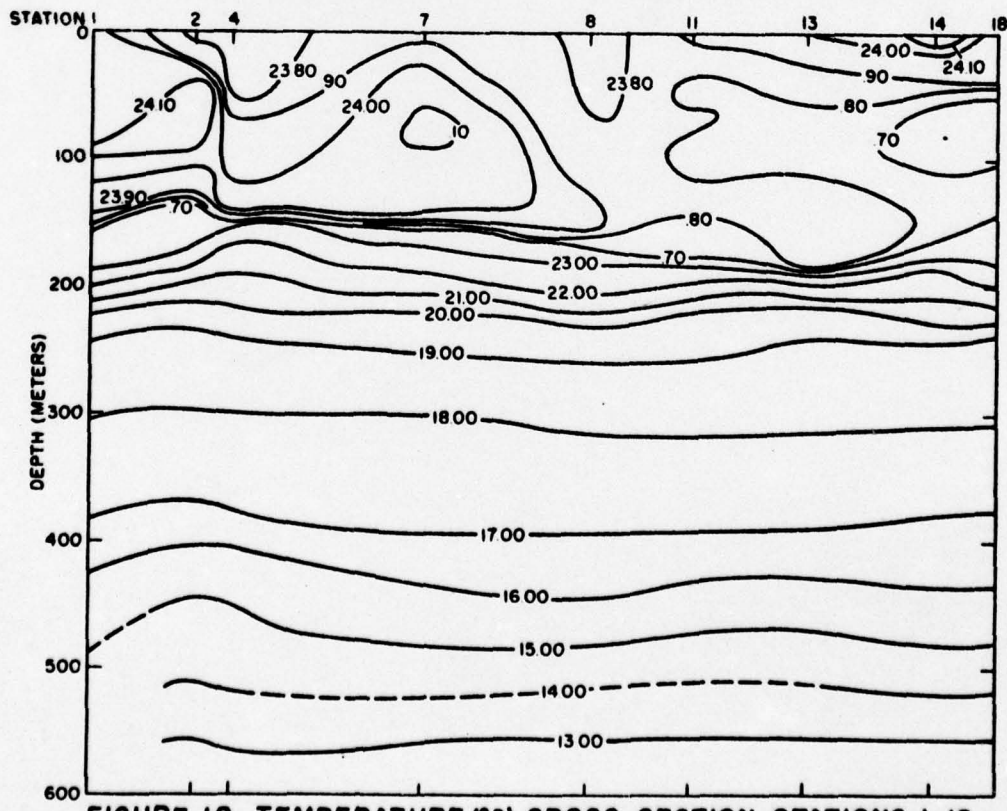


FIGURE 10 TEMPERATURE (°C) CROSS SECTION STATIONS 1-18

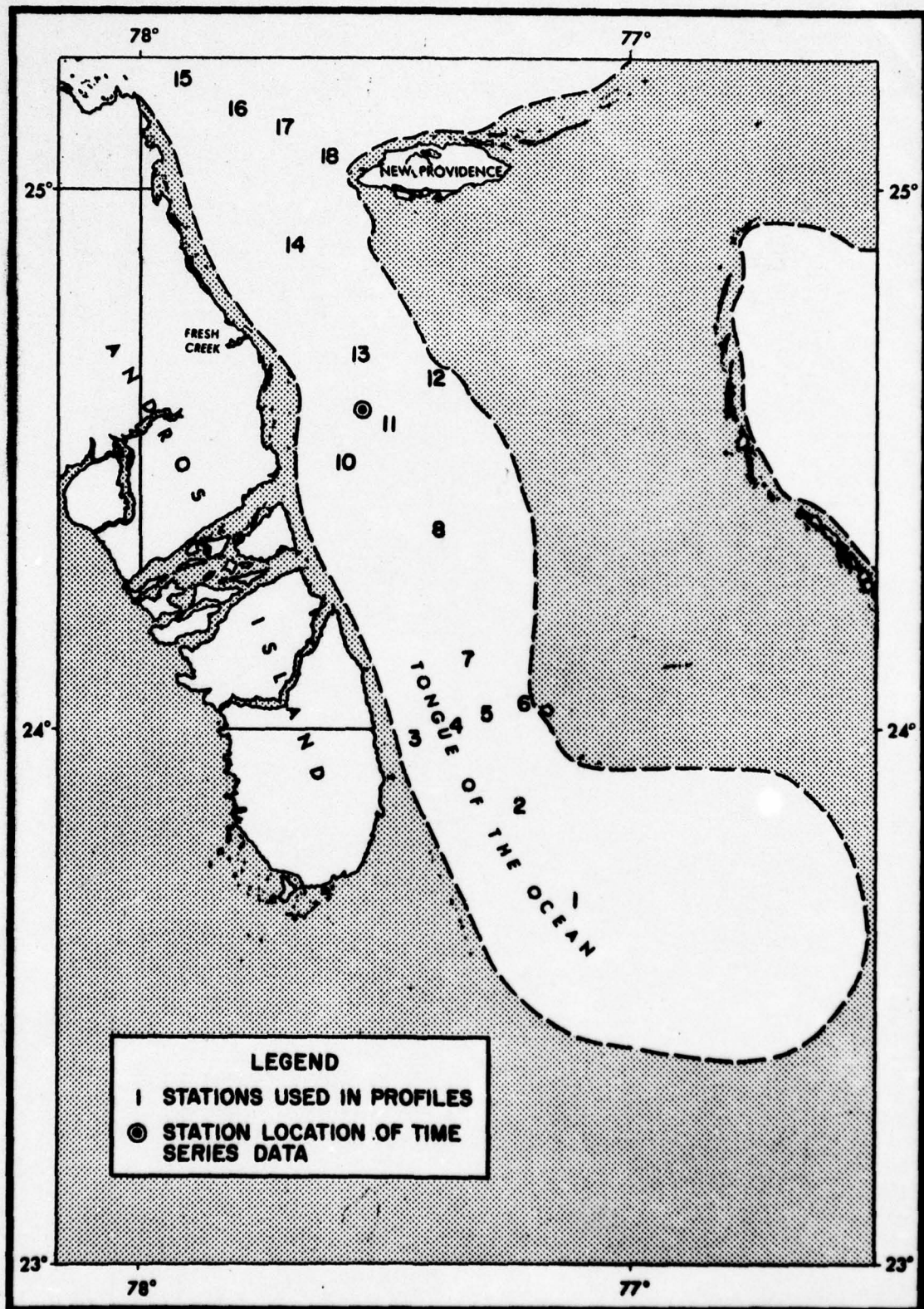


FIGURE II STATION LOCATIONS

Table I Results of Run No. 1

Sample No.	Time (local)	Depth to Bottom (fms)	Sample Depths		Salinity (°/oo)	Temperature (°F)
			S = surface	B = bottom		
1	0955	3 1/2	S	B	37.33	76.8
2	1045	3 1/2	S	B	37.51	77.0
3	1100	3 1/4	S	B	37.51	77.0
4	1115	3 1/4	S	B	37.41	77.5
5	1130	3	S	B	37.43	
6	1145	3	S	B	37.38	77.5
7	1215	3	S	B	37.38	
8	1245	3	S	B	37.45	78.0
9	No Samples				37.46	
10	No Samples				37.59	78.0
11	1330	3	S	B	37.56	
12	1400	2 1/2	S	B	37.31	78.0
13	1430	2 3/4	S	B	37.38	
14	1500	2 3/4	S	B	37.32	79.0
15	1530	2 3/4	S	B	37.31	
16	1630	3 1/2	S	B	37.35	78.0
					37.33	
					37.30	
					37.37	78.0

Note: Depths were determined by lead line and were not corrected for the stage of the tide. Temperatures were measured by bucket thermometer. Station locations are shown on Figure 12.

Table II Results of Run No. 2

Sample No.	Time (local)	Depth to Bottom (fms)	Sample Depths S = surface B = bottom	Salinity (°/oo)	Temperature (°F)
1	0800	4 1/2	S	37.01	77.0
2	0820	3 1/2	B	36.99	
3	0845	3 1/2	S	36.98	77.0
4			B	36.96	
5	0915	3	S	36.96	77.4
6	0930	3	B	36.96	
7	0945	2	S	36.97	
8	1000	2 1/2	B	37.01	77.0
9	1015	2 1/2	S	36.99	
10	1025	2 1/2	B	37.01	77.0
11	1055	2 1/2	S	37.02	
12	1105	2 1/2	S	37.05	77.0
13	1155	2 1/2	B	37.05	
14	1215	3	S	37.06	77.5
15	1230	3	B	37.02	
16	1245	3	S	36.98	78.0
17	1300	3	B	36.97	
18	1315	3 1/2	S	36.96	77.1
19	1330	3	B	36.97	
20	1345	4 1/2	S	36.90	77.5
21	1400	5	B	36.94	
			S	36.92	77.5
			B	36.91	
			S	36.92	77.6
			B	36.94	
			S	36.92	77.6

Note: Depths were determined by lead line and were not corrected for the stage of the tide. Temperatures were measured by bucket thermometer. Station locations are shown on Figure 12.

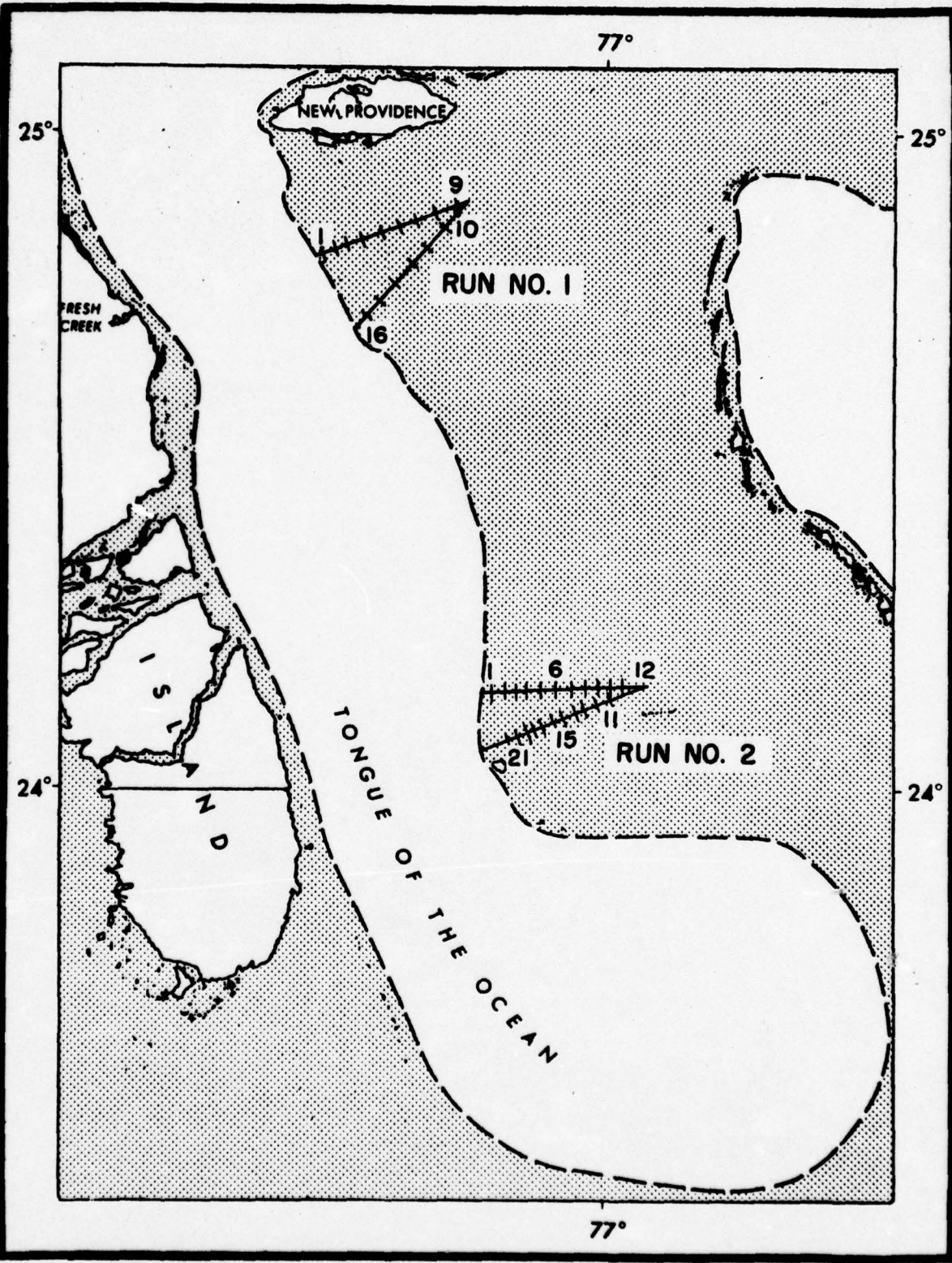


FIGURE 12 TRACK OF SHALLOW WATER SAMPLING RUNS

Salinity

The TOTO is located in a region where evaporation from the sea surface probably exceeds precipitation. Consequently, the TOTO becomes a quasi-evaporation basin where salts are being concentrated in the sea water. Recent observations within the shoal areas east of the TOTO show salinity values which vary from 37.5 ‰ just south of New Providence Island to about 37.0 ‰ just north of Green Cay. Figure 12 shows the tracks followed during two excursions onto the banks east of the TOTO. Tables I and II present the results of data collected during Run No. 1 and Run No. 2, respectively. There is evidence that some high salinity water enters the cul-de-sac from the surrounding shoals. These shoal waters also have an important environmental effect on the main body of the TOTO. A computation of σ_t based on a temperature of 77.0°F (25.0°C), as measured by bucket thermometer, and a salinity of 37.5 ‰ shows that the density of the shoal water equaled that found at about 175 meters in the central TOTO. The intrusion of this bank water has a very pronounced effect upon the thermo-haline circulation. In fact, historical data have shown that isolated patches of anomalously high salinity water can be found intermittently throughout the TOTO (Fig 16). Such lenses would significantly affect sound propagation.

Horizontal and longitudinal salinity profiles are presented in Figures 13 through 16. These profiles are based on data collected during March 1960. Station locations are shown in Figure 11.

Time Variations

Data have been collected from anchored ships to examine possible time variations of physical properties at a point in the TOTO. These data

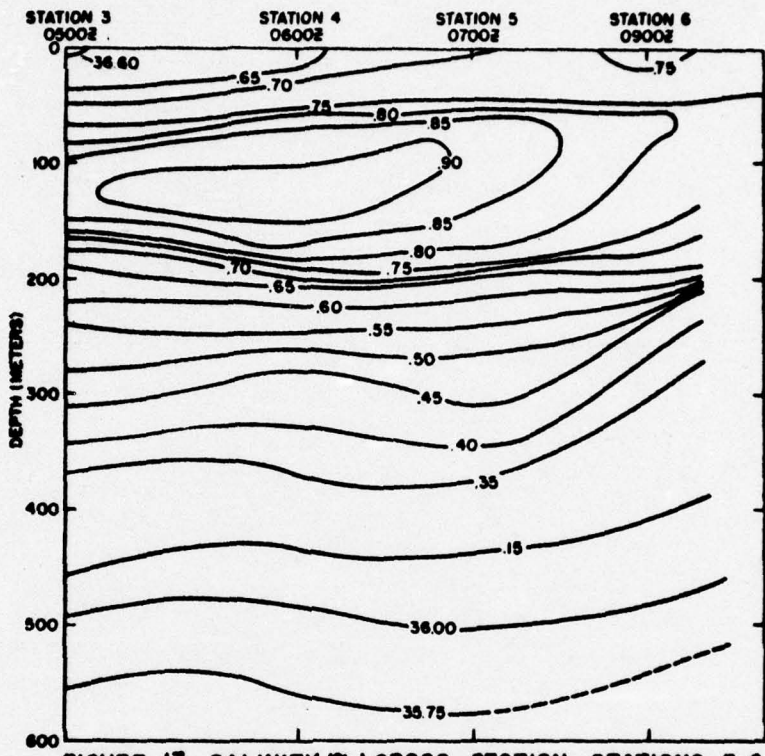


FIGURE 13 SALINITY (‰) CROSS SECTION STATIONS 3-6
16 MARCH 1960

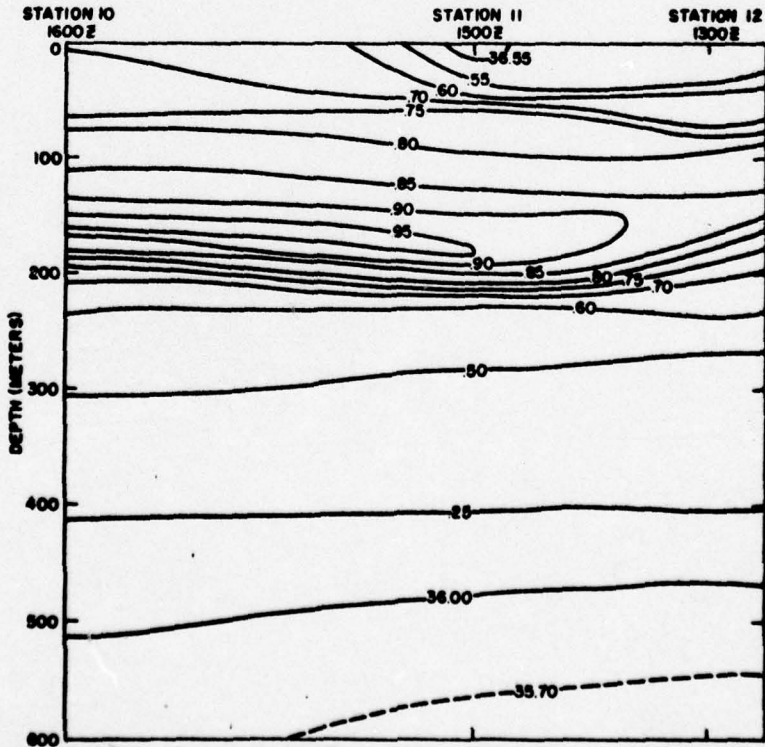


FIGURE 14 SALINITY (‰) CROSS SECTION STATIONS 10-12
18 MARCH 1960

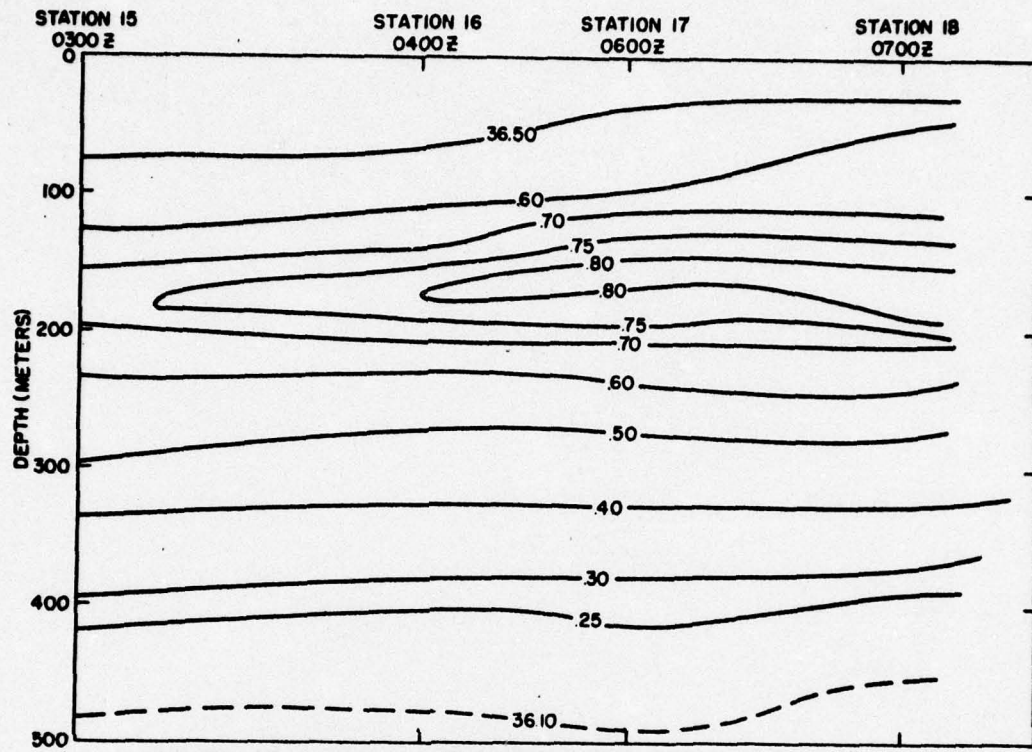


FIGURE 15 SALINITY(‰)CROSS SECTION STATIONS 15-18
19 MARCH 1960

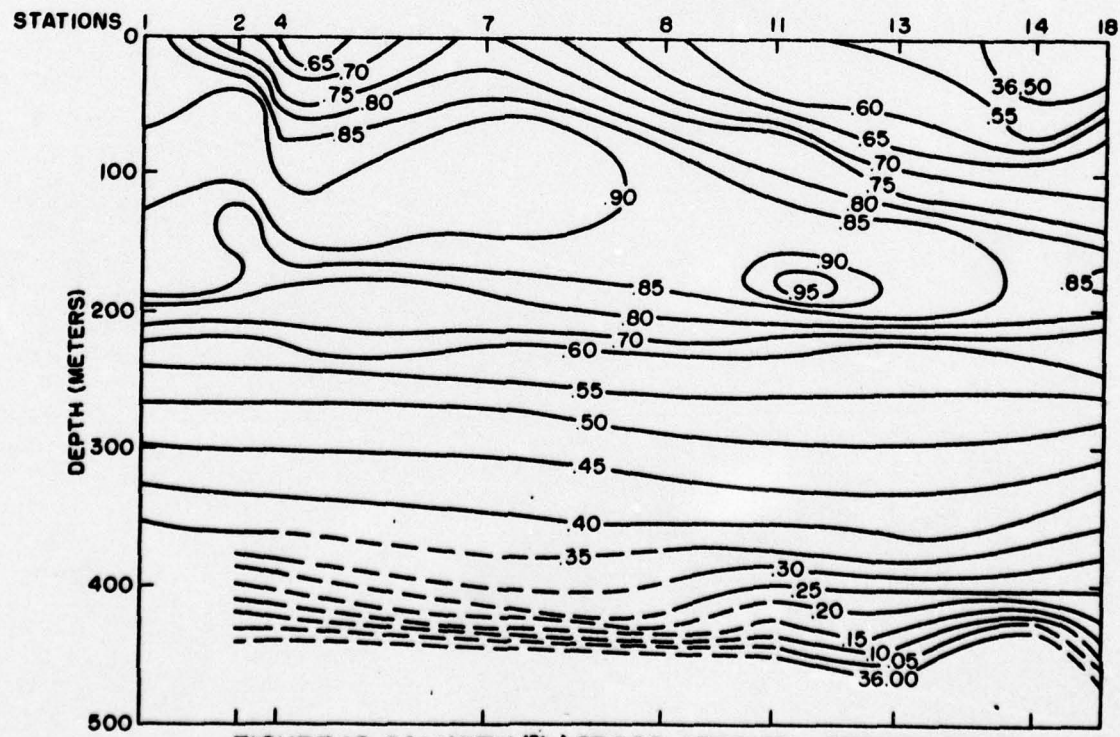


FIGURE 16 SALINITY (‰) CROSS SECTION STATIONS 1-18

Indicate that very large changes in physical properties may occur in relatively short time intervals. For example, data collected over a period of 3 days at latitude $24^{\circ} 39'N$, longitude $77^{\circ} 35'W$ during December 1961 revealed that at 200 meters the temperature showed a mean decrease of about $2^{\circ}C$. Superimposed upon the general decrease were oscillations which were apparently caused by a combination of a force with a period nearly equal to that of the tide and other forces of undetermined periods. Throughout the period of observation a nearly constant 20-knot wind was blowing with a modal direction of 45° to 54° with directions ranging between 0° and 90° True. Wind stresses could cause aperiodic variations in depths of various isolines.

These are several forces occurring in nature which could generate the types of oscillations observed in the TOTO. Two of the most suggestive are discussed below.

Horizontal Advection

The following discussion is based on the use of rectangular coordinates with the X axis along the line connecting Stations 1 and 17 of Figure 11 and the Z axis positive downward. Assuming diffusive transport to be negligible, the equation which represents the time change of a property, T, of sea water can be written as

$$\frac{dT}{dt} = \frac{\partial T}{\partial t} + v_x \frac{\partial T}{\partial x} + v_y \frac{\partial T}{\partial y} + v_z \frac{\partial T}{\partial z}.$$

Over a long time $\frac{dT}{dt} \approx 0$, and if the vertical component of velocity is small compared to v_x and v_y , then the local change in a property can be written as

$$-\frac{\partial T}{\partial t} = v_x \frac{\partial T}{\partial x} + v_y \frac{\partial T}{\partial y}.$$

The local change $\frac{\partial T}{\partial t}$ and the horizontal gradients can be evaluated from observations.

The conservative property selected is temperature. The observations upon which these calculations are based were made simultaneously from 3 anchored vessels. The local change and the horizontal gradients are

$$\frac{\partial T}{\partial t} = 0.33^\circ\text{C/hr}, \quad \frac{\partial T}{\partial x} = 0.06^\circ\text{C/mile},$$

$$\text{and} \quad \frac{\partial T}{\partial y} = 0.08^\circ\text{C/mile}.$$

The resulting equation is

$$0.33^\circ\text{C/hr} = v_x 0.06^\circ\text{C/mile} + v_y 0.08^\circ\text{C/mile}. \quad (1)$$

The relative magnitudes of the components of v are not known, but for computational purposes it is assumed that the component of velocity associated with the largest gradient, v_y , is twice the other component; thus, in a sense, the value of v is minimized.

Solving equation (1) yields $v_x = 1.5$ knots, $v_y = 3.0$ knots, and $|v| = 3.3$ knots. The mean tidal current speed from slack to slack is about 0.6 of the maximum speed. Consequently, currents of about 5 knots would occur in the TOTO if the horizontal advection were producing the observed changes. Currents of this magnitude have not been observed in the TOTO.

Internal Waves

The classical approach to a discussion of the internal wave phenomena assumes a two-layered ocean, the upper layer having a density ρ^1 and thickness h^1 ; the lower having a density ρ and depth h . At the boundary between these two layers, waves may occur which are quite different from those appearing on the free surface of the ocean. Because these waves occur

within the medium or at the boundary between the two layers of the medium, they are termed internal or boundary waves. The amplitudes of these waves are usually considerably larger than that of surface waves. The principal characteristics of these waves are that maximum amplitudes occur within the boundary layer, with amplitudes decreasing in either direction from this layer.

In the presence of internal waves, there are accompanying variations in physical properties of the medium which also at times may be quite large. Figure 17 shows the time variation in temperature at indicated depths in the northern TOTO. These data were collected from an anchored ship at latitude $24^{\circ} 35'N$, longitude $77^{\circ} 35'W$ during March 1962. The observations show the amplitude of variation in temperature is largest near the boundary layer (thermocline) where the vertical gradient of temperature is maximum (200 to 300 meters). It follows (see equation below) that in order for the wave amplitudes to be maximum within this layer (as predicted by theory), then the deviation from a depth mean of temperature must also be maximum. For example, over a six-hour period at 200 meters the temperature changed by about 1.8°C . Variations of this magnitude were not observed outside this depth range. These variations would have a considerable affect on sound propagation. For example, with a salinity of 36 ‰ a temperature change of 1.8°C would produce a change in sound velocity of about 4.5 m/sec. However, there are certain characteristics of internal waves which makes the study of the wave itself important. For example, relatively large instantaneous particle velocities may be associated with these waves. These velocities may have a considerable affect upon trajectories of underwater projectiles.

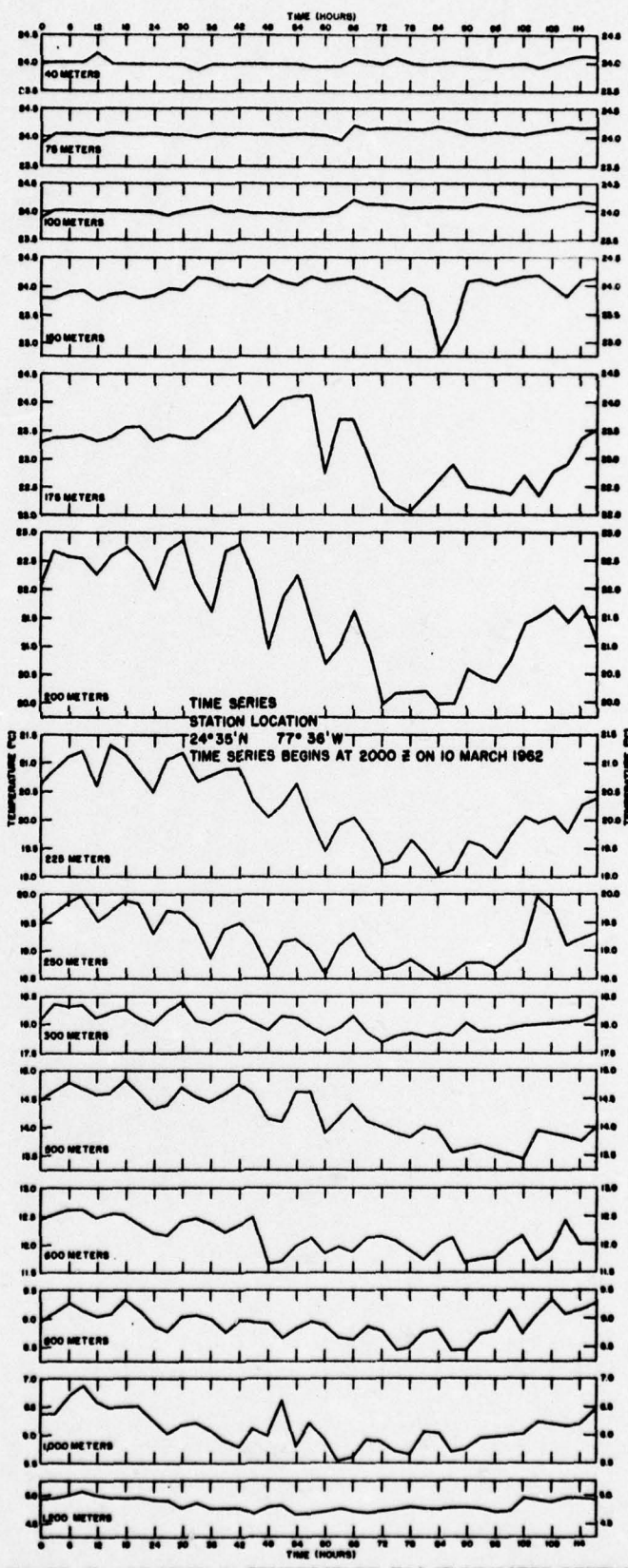


FIGURE 17 VARIATION IN TEMPERATURE (°C) AT INDICATED DEPTHS

If properly spaced observations of a conservative property of the medium are available, then computations may be made which determine the amplitudes of the internal waves. The amplitude, η , may be computed from the relationship

$$\eta = \frac{T^1}{\frac{dT}{dz}}$$

where T^1 is the deviation from the time mean temperature \bar{T} . Figures 18 through 23 illustrate the results of such computations for selected depths based on an observation period of 135 hours. These computations are based on the same data that appears in Figure 17.

The condition of a homogeneous upper layer of density ρ^1 and a homogeneous lower layer of density ρ is rarely encountered in the deep ocean areas. Instead, the in situ density increases continuously with depth. Fjeldstad (1935) has developed a theory of internal waves in a medium in which the density is a continuous function of depth. The theory predicts the possible existence of an infinite number of internal waves of the same period, but with different vertical distribution of vertical displacements. These waves are designated as waves of first order, second order, etc. The wave of zero order is the surface wave. The wave of first order is characterized by the fact that vertical displacements from the surface to the bottom have the same sign and a maximum amplitude at a single depth. The wave of second order has vertical displacements which are opposite in sign between the upper and lower layers (although the depth distribution of density is assumed continuous, layers have to be defined in accomplishing computations), and there are two maxima. The wave of third order has three maxima, etc. These waves are further characterized by the fact that the horizontal velocities are maximum where the vertical amplitude is zero.

NOTE: GRAPHS ARE BASED ON DATA SHOWN ON FIGURE 17

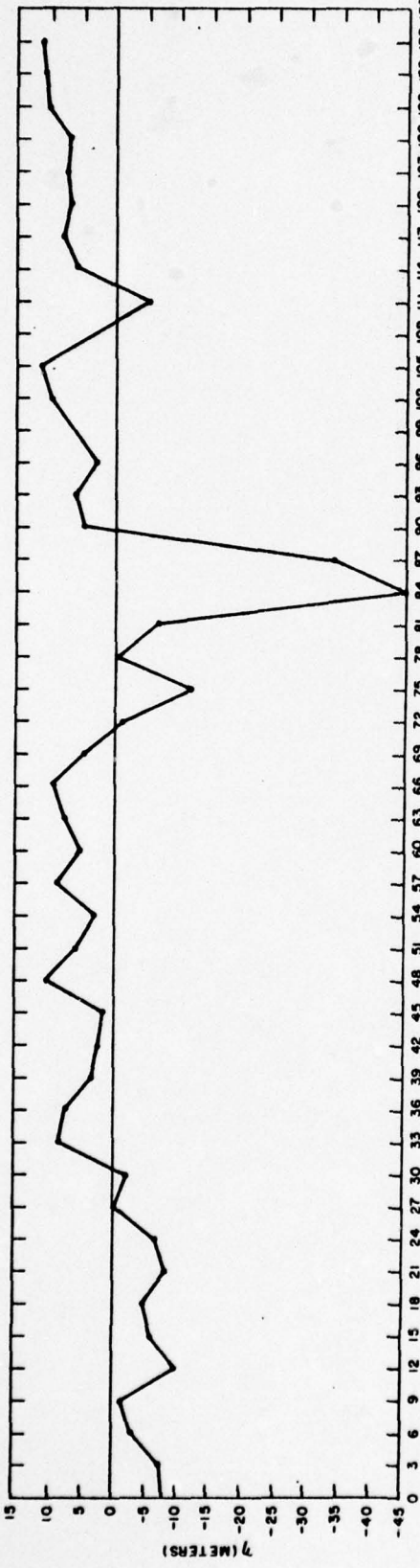


FIGURE 18 RESULTS OF COMPUTATIONS OF $T \cdot \frac{1}{d^2}$ AT $z = 150$ METERS

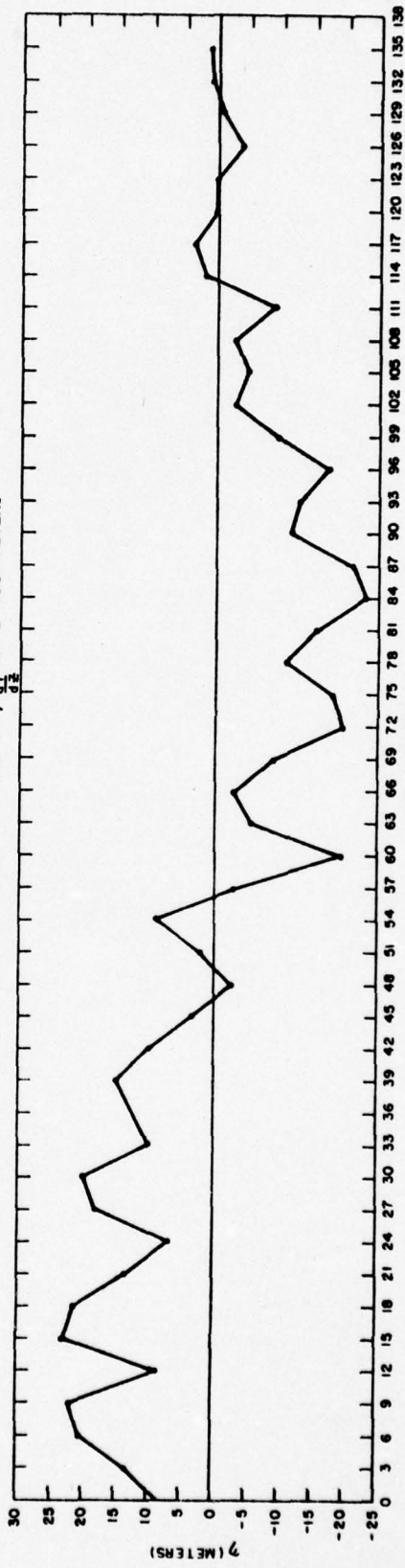


FIGURE 19 RESULTS OF COMPUTATIONS OF $T \cdot \frac{1}{d^2}$ AT $z = 225$ METERS

NOTE: GRAPHS ARE BASED ON DATA SHOWN ON FIGURE 17

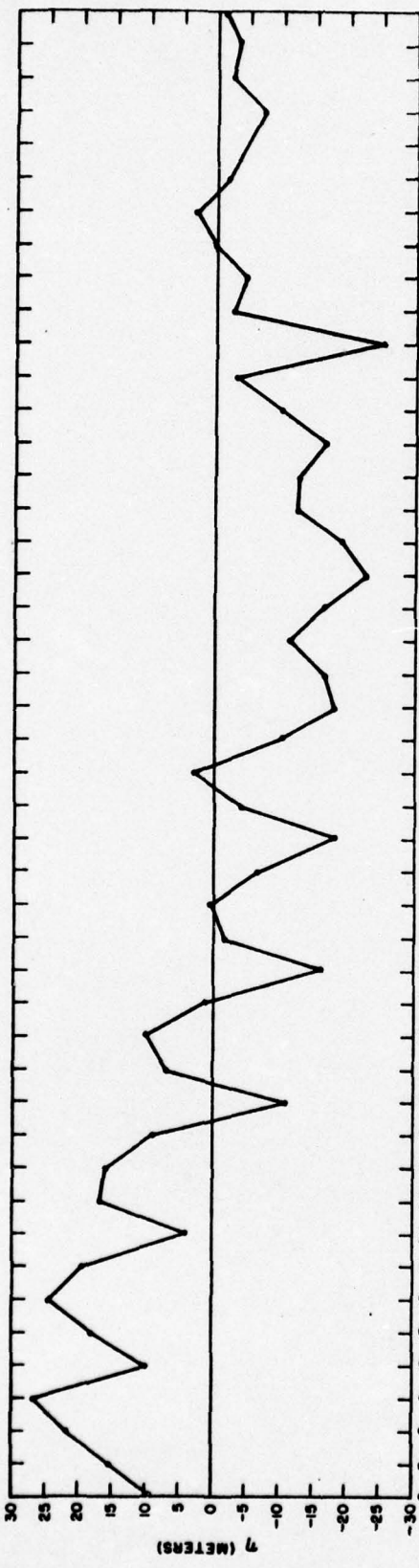


FIGURE 20 RESULTS OF COMPUTATIONS OF $\eta = \frac{T}{\sqrt{2}} \sin \left(\frac{\pi t}{T} \right)$ AT $z = 250$ METERS

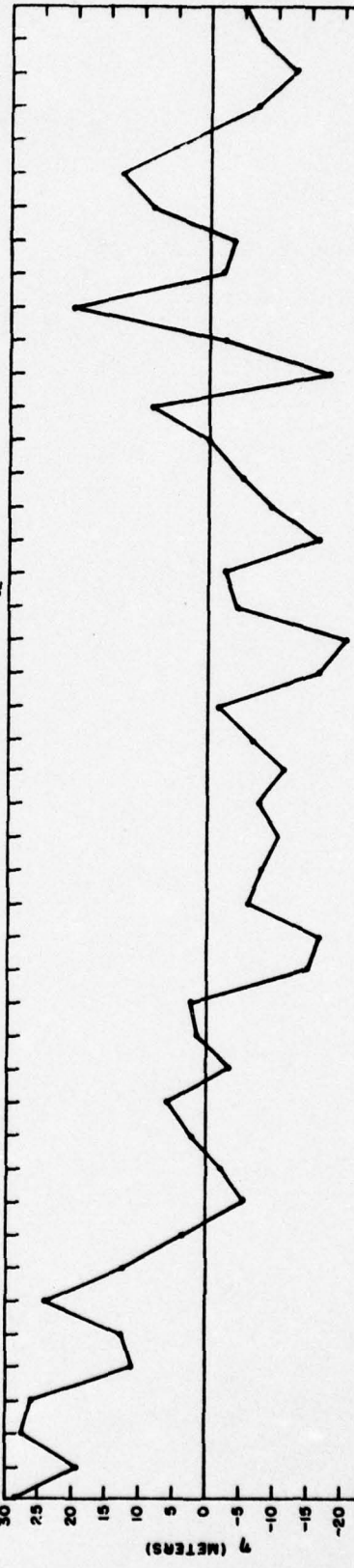


FIGURE 21 RESULTS OF COMPUTATIONS OF $\eta = \frac{T}{\sqrt{2}} \sin \left(\frac{\pi t}{T} \right)$ AT $z = 500$ METERS

NOTE: GRAPHS ARE BASED ON DATA SHOWN ON FIGURE 17

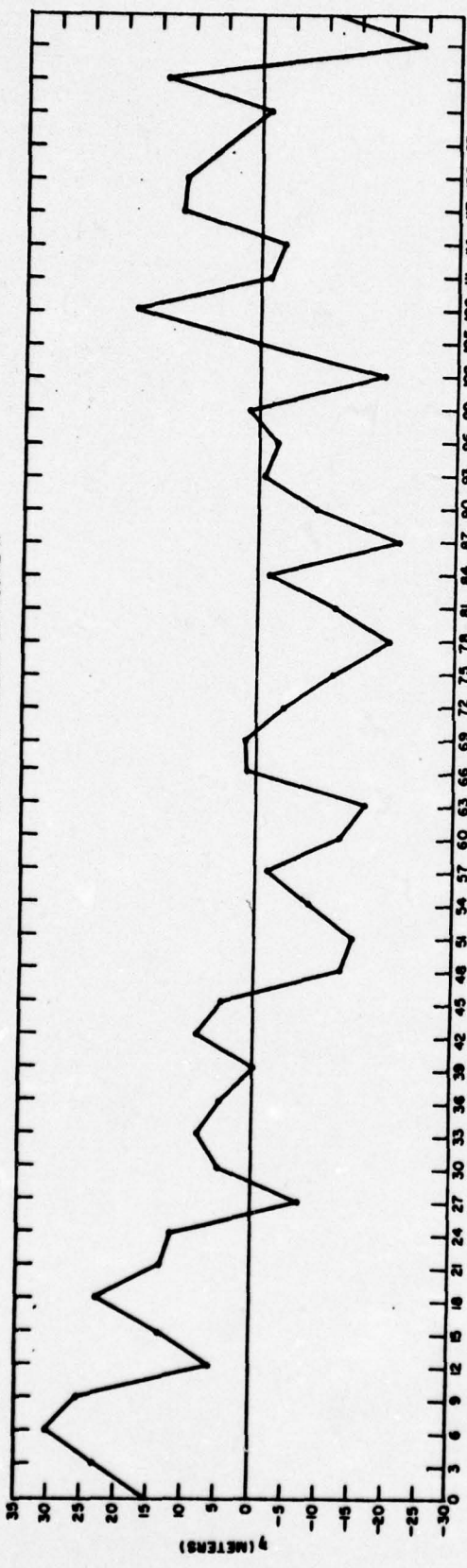


FIGURE 22 RESULTS OF COMPUTATIONS OF $\gamma = \frac{T}{1-T}$ AT $z = 700$ METERS

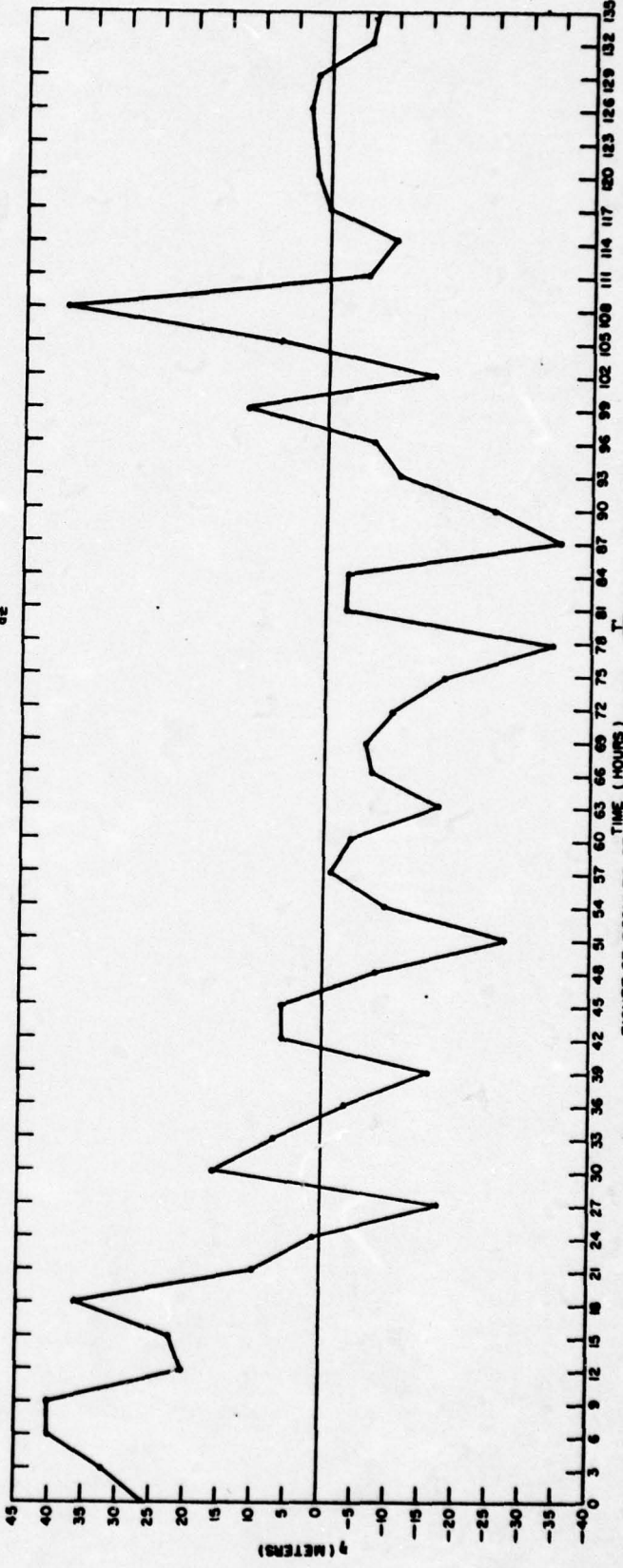


FIGURE 23 RESULTS OF COMPUTATIONS OF $\gamma = \frac{T}{1-T}$ AT $z = 750$ METERS

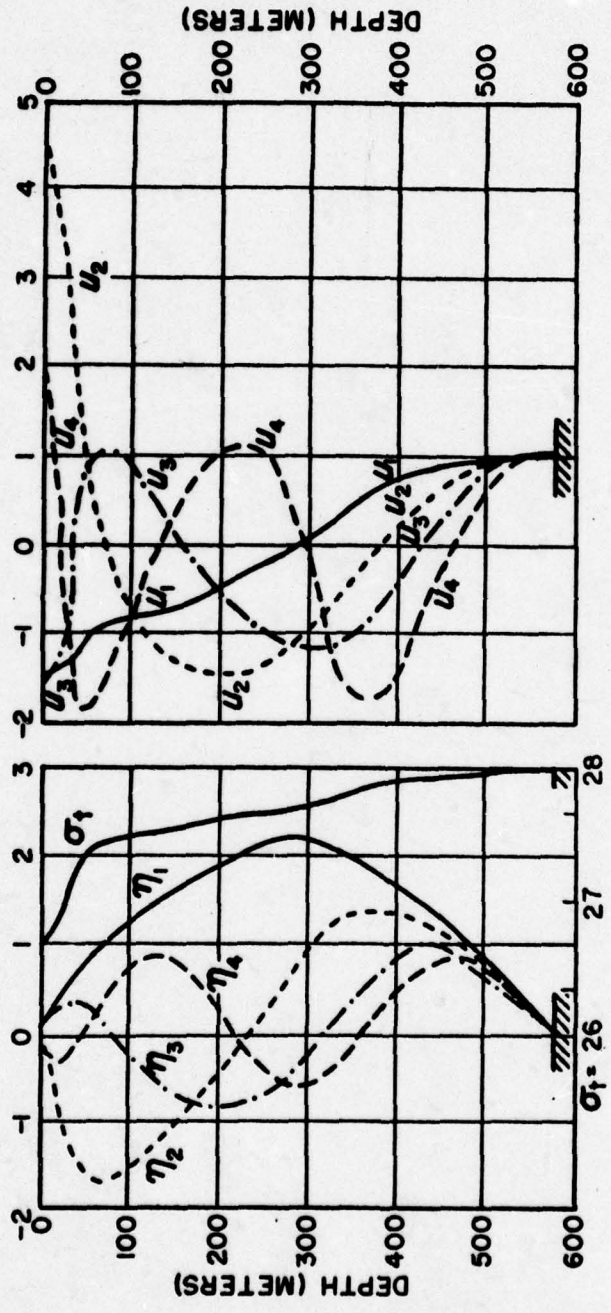


FIGURE 24 INTERNAL WAVES

LEFT: VERTICAL DISTRIBUTION OF THE DENSITY σ_1 AND VERTICAL DISTRIBUTION OF THE VERTICAL DISPLACEMENTS η OF THE INTERNAL WAVES OF THE 1ST UNTIL 4TH ORDER AT THE "MICHAEL SARS" STATION 115. RIGHT: VERTICAL DISTRIBUTION OF THE AMPLITUDES OF THE HORIZONTAL VELOCITIES CORRESPONDING TO THE INTERNAL WAVES OF THE 1-4TH ORDER. η AND u ARE IN ARBITRARY UNITS.
(FJELDSTAD)

Figure 24 (from Defant, 1961) shows σ_t and vertical displacements of horizontal velocities associated with the vertical oscillations. It should be noted that since the amplitude of the vertical displacements of all orders is necessarily zero, the horizontal velocities must all reach a maximum near the bottom. This condition could produce significant oscillatory flow. Bottom photographs taken at depths of about 1,700 meters in the TOTO show very distinct parallel ripple marks which may have resulted from such a flow.

Meteorological Influences

Meteorological elements must also be considered in attempting to define changes such as those observed in the TOTO. For example, a strong persistent wind will produce a temporary pile-up of water along a coastline of the TOTO. When wind speeds subside the water will then undergo a period of dynamic readjustment. In an enclosed body, the manifestation of such readjustments may be oscillations of isolines of various properties such as those exhibited in the TOTO. These oscillations would be superimposed upon any permanent oscillations present in the TOTO. They would have a period dependent upon the geometry of the enclosed body of water and an amplitude varying with the amount of pile-up.

The period of a free oscillation of a basin open at one end can be approximated from the relationship

$$T = \frac{4L}{\sqrt{gh}}$$

where T = period, L = length, h = depth, and g = gravity.

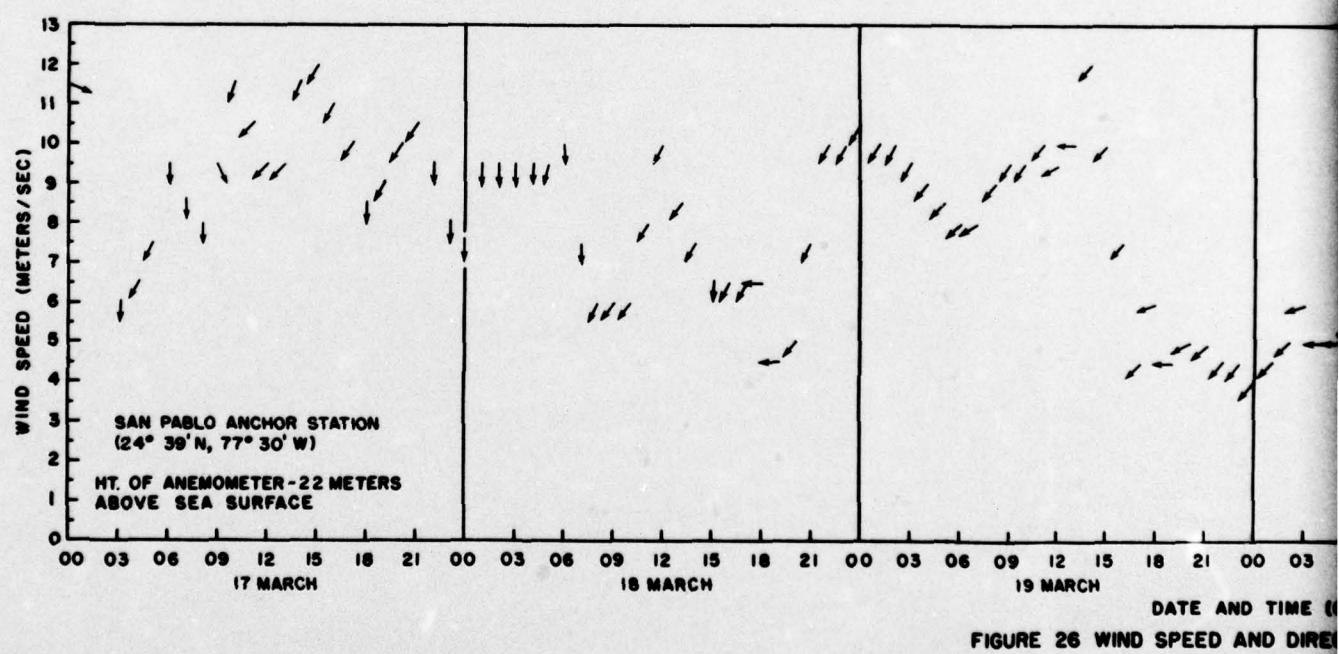
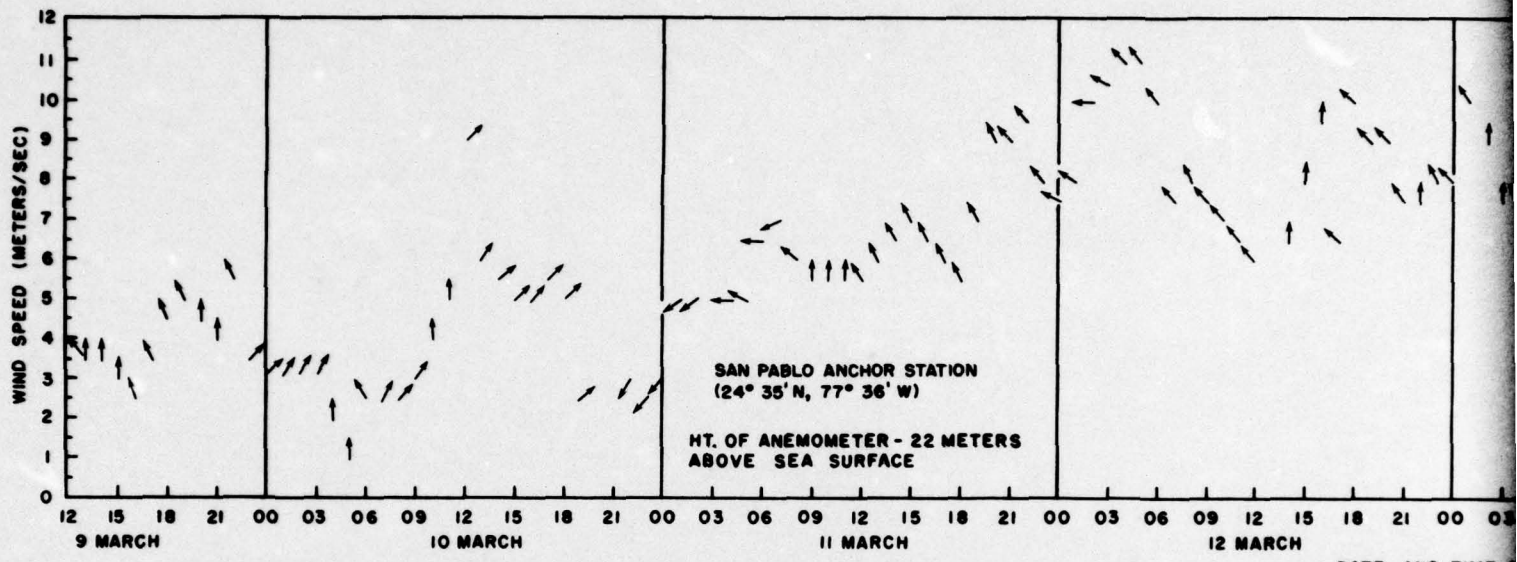
The period of a transverse oscillation in the TOTO can be best approximated by the period of oscillation of a closed basin. The period is given by

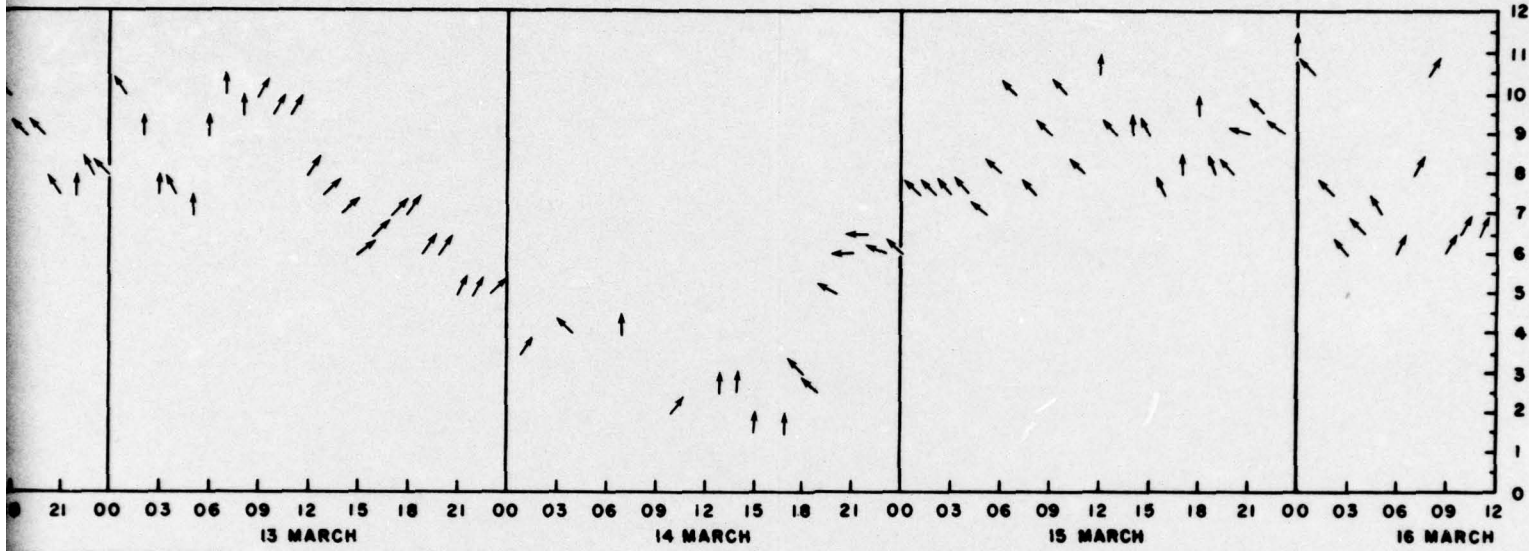
$$T = \frac{2L}{\sqrt{gh}}.$$

Those oscillations which occur along the length of the TOTO are likely to lose energy through the northern opening and, therefore, dissipate quickly. However, transverse oscillations will be evident for a longer time because they are likely to be reflected back and forth across the TOTO until the energy is dissipated by friction.

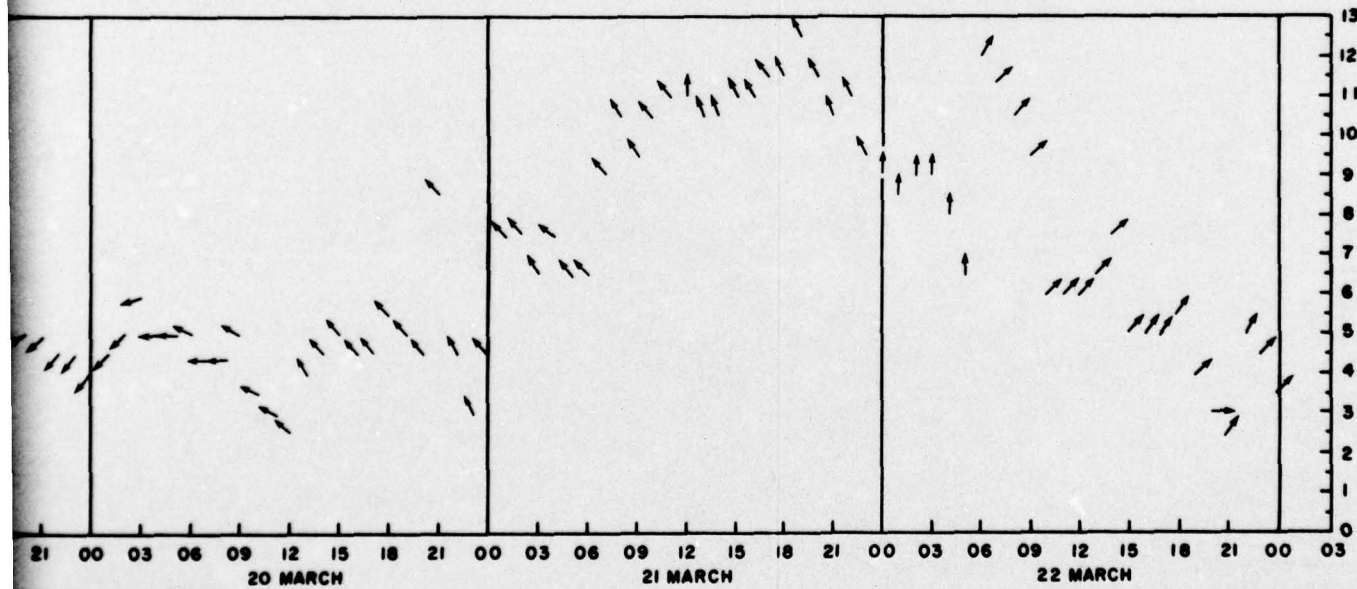
The length of the TOTO was measured from 25°N latitude to Queens Channel in the cul-de-sac on H. O. Chart 26-B. Assuming the chart scale at 26°N to be applicable to the length of the TOTO, the measurement shows a length of 102 nautical miles. Using an average depth of 1,000 fathoms and a width of 25.5 nautical miles, the resulting transverse oscillation is about 12 minutes and the longitudinal oscillation is about 96 minutes. Observations have not been made which allow an inspection of such short periods.

The effect of wind stresses on the surface of the water may also become evident through vertical displacements of various isopleths with time (Defant, 1961). During the March 1962 survey operations in the TOTO, hourly observations of wind speed and direction were made. These data were plotted (Fig 25 and 26) in an attempt to establish some correspondence between large variation in depth of an isopleth and the occurrence of abnormally strong winds or a sudden shift in wind direction. Figures 27 and 28 show the variation with time of the thickness of the mixed layer (as defined previously) and the depth of selected isotherms. The data show that maximum depression of an isothermal surface and deepening of the mixed layer can be associated with periods of sustained strong (>7 m/s) winds. These variations in wind speeds appear to be cyclic. The differential heating of Andros Island, which is a considerable land mass, and the surrounding waters might account for the cyclic variation in wind speeds.





DATE AND TIME (GMT)
AND DIRECTION - SAN PABLO - 9-16 MARCH 1962



WE AND TIME (GMT)
WIND AND DIRECTION-17-22 MARCH 1962

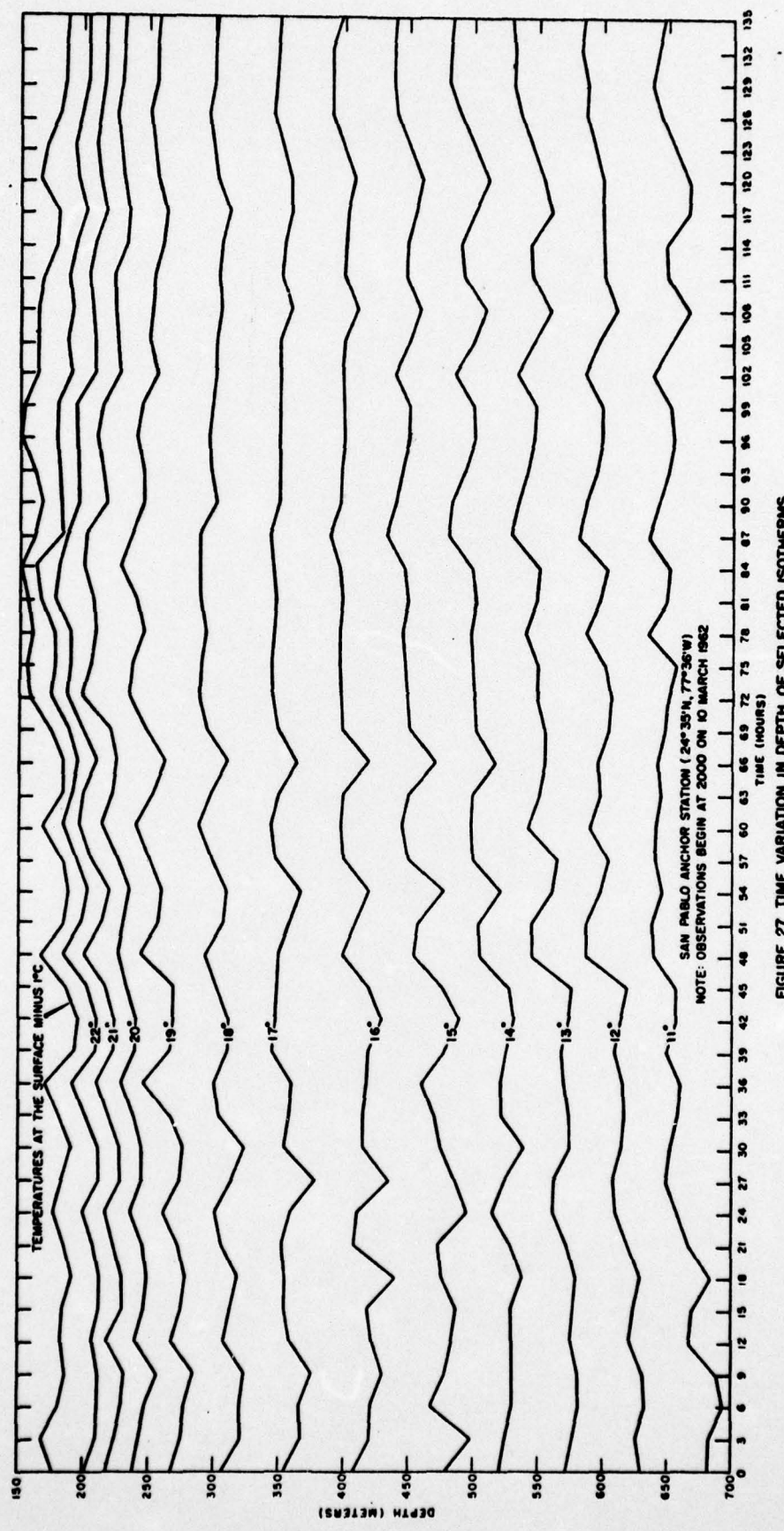


FIGURE 27 TIME VARIATION IN DEPTH OF SELECTED ISOTHERMS

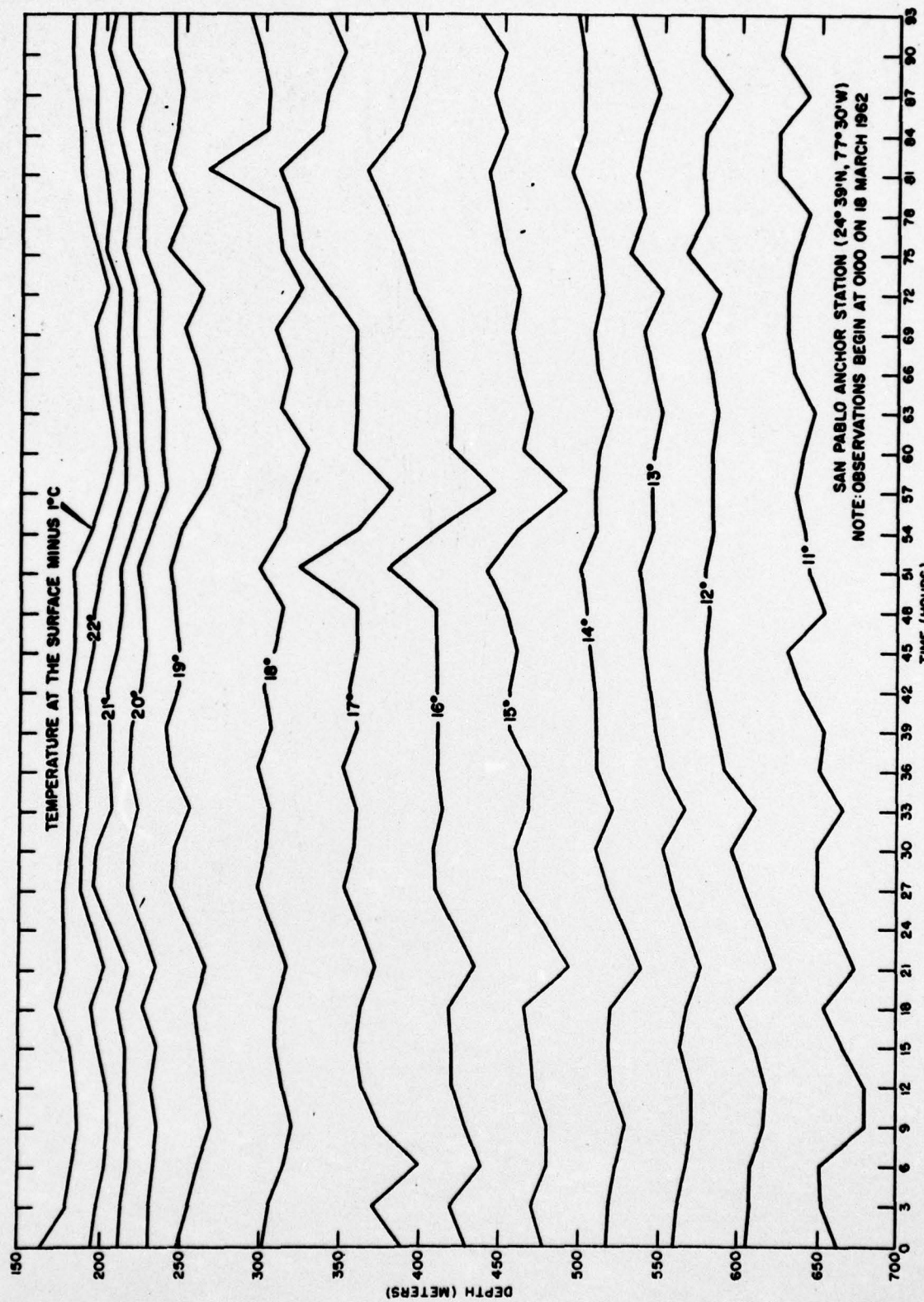


FIGURE 28 TIME VARIATION IN DEPTH OF SELECTED ISOTHERMS

The main consideration here is that winds are a possible source of energy required to produce the vertical oscillations observed in the TOTO. Future surveys in the TOTO will be planned to detect these findings.

Stability

If a particle of sea water is subject to vertical displacement, then the particle may no longer be in equilibrium with its new environment. For example, if a particle A moves downward, reaching B (Fig 29), the temperature of the particle grows adiabatically by a magnitude designated as $d\zeta$. The resulting change in density will be $\frac{\partial \rho}{\partial t} d\zeta$. The density of A, which was originally at depth z, at depth $z + dz$ then becomes

$$\rho_{s,t} \rho + d\rho + \frac{\partial \rho}{\partial t} d\zeta.$$

If particle A is lighter than the particles at B, then A will tend to rise; if A is heavier than the particles at B, then A will continue to sink; if the particles A and B are equal in density, then A will remain at B.

The difference in density

$$\delta\rho = (\rho_{s+ds, t+dt, P+dP}) - (\rho_{s,t,P} + \frac{\partial \rho}{\partial t} d\zeta)$$

represents a measure of vertical stability between a depth of z and $z + dz$. The water over this interval will be stable, indifferent, or unstable depending upon whether $\delta\rho \gtrless 0$.

The expression for stability, E, as derived by Hesselberg and Sverdrup is

$$E = \frac{\partial \rho}{\partial t} \left[\frac{dt}{dz} - \frac{d\zeta}{dz} \right] + \frac{\partial \rho}{\partial s} \frac{ds}{dz}$$

where ζ = adiabatic temperature, t = in situ temperature, s = salinity, and ρ = density.



$$\rho_A = \rho_{s,T,P+dP} + \frac{\partial \rho}{\partial T} dT$$

$$\delta \rho = \rho_B - \rho_A$$

FIGURE 29 CHANGE IN DENSITY CAUSED BY A VERTICAL
MIGRATION dZ

The more conventional relationship $E = \frac{d\sigma_t}{dz}$ was not used because of the relative magnitude of the vertical salinity gradient. In the TOTO $\frac{ds}{dz}$ is very much different from zero and cannot be neglected in determining stability.

The terms $\frac{dt}{dz}$ and $\frac{ds}{dz}$ can be evaluated from observations. Hesselberg and Sverdrup have published tables which allow the determination of the remaining terms for computing E. The accuracy of these determinations is also discussed by the above authors. Figures 30 and 31 present the results of computations using the same data as used in constructing the T-S curves of Figures 2 and 4.

The computations for March (Fig 30) show a weakly unstable surface layer to about 65 meters. The stability shows a maximum at about 120 meters, but a very pronounced maximum exists at about 225 meters. A third less pronounced maximum occurs at about 600 meters.

The curve for September (Fig 31) shows two very pronounced maxima above 200 meters. The first, and larger, occurs at about 65 meters and the second at about 180 meters. The increase in stability at 65 meters in September relative to March is the result of summer heating and consequent thermal stratification. The maximum at 600 meters is only weakly apparent in September, but a very pronounced maximum exists at 1,000 meters.

The curves indicate that the TOTO may have four very definite layers by the end of the summer season. With the advent of winter, the intense thermal stratification at about 65 meters will disappear, and maximum stability will again occur at a depth of about 200 meters. These curves also indicate the possible dangers of mixing data of various seasons. It may be of interest to mention a set of computations that were made (but not

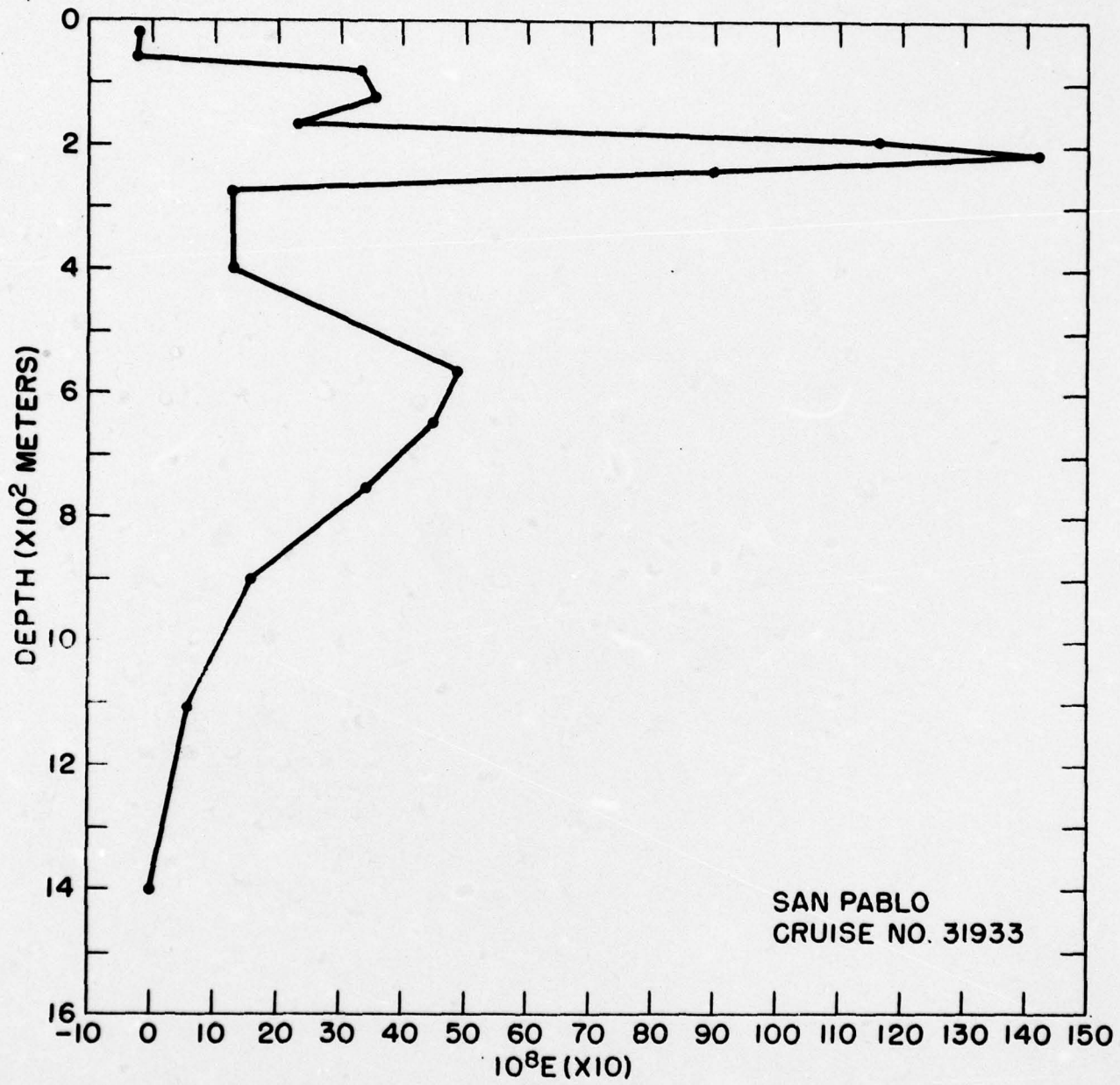


FIGURE 30 STABILITY VS DEPTH - MARCH 1962

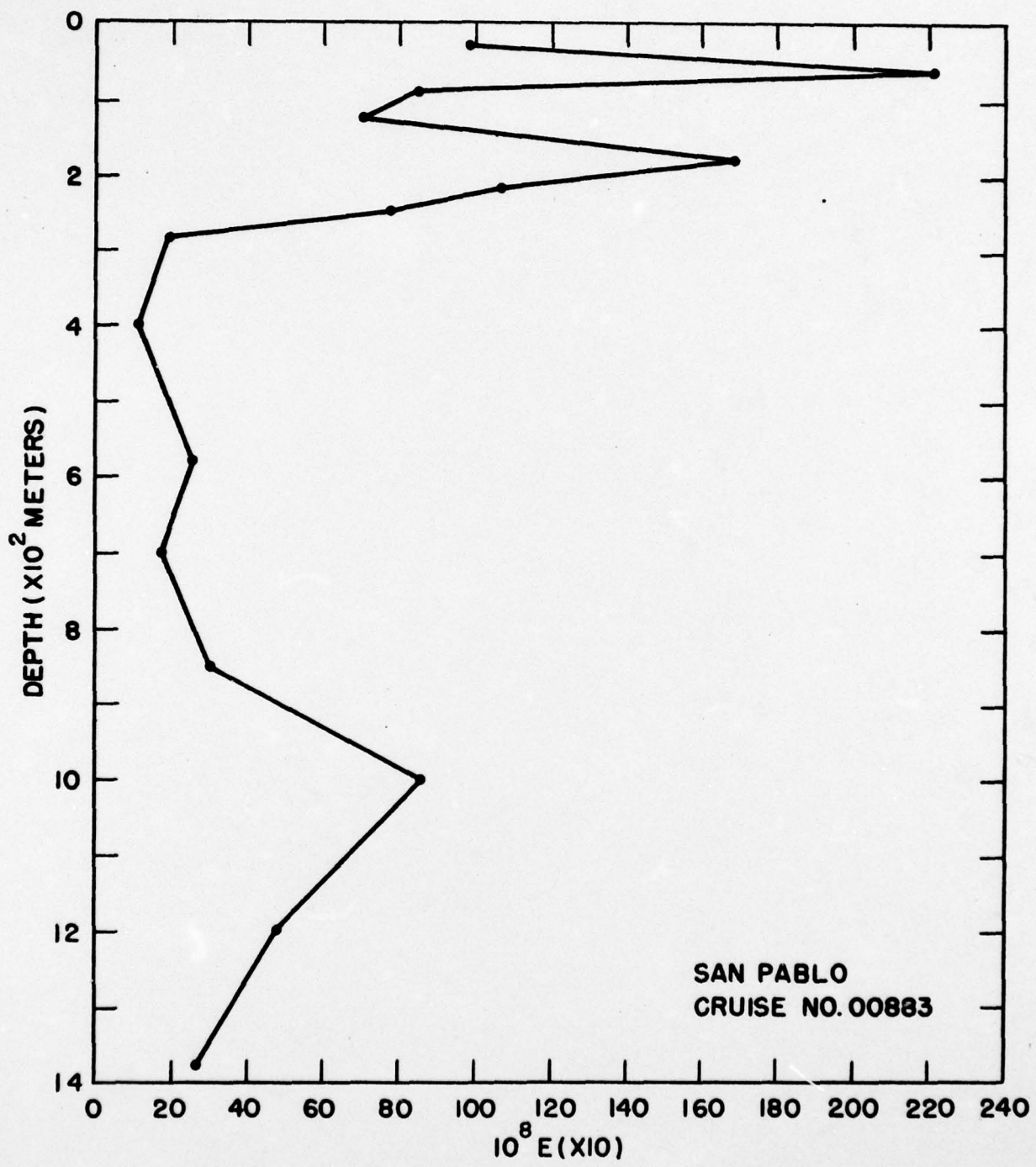


FIGURE 31 STABILITY VS DEPTH - SEPTEMBER 1961

presented in this report) using all data available for a small area regardless of season. Standard deviations of temperature were computed for several depths. These computations indicated maximum variations at 200, 500 to 600, and 800 to 1,000 meters, whereas the stability curves indicate a single maximum below 300 meters during March with only a slight maximum appearing at 500 to 600 meters during September. These curves indicate that relatively stable layers, and consequently possible internal oscillations, will exist at different depths during different seasons. It is believed that the stability parameter can be used as an indicator for the depth of occurrence of internal oscillations.

Tides

Little meaningful tide data for the TOTO are available. The tide is semidiurnal with some diurnal inequality occurring primarily in the low waters. The data which are available indicate that high water occurs from New Providence Island to Green Cay and Pigeon Cay within a 30-minute period. Available records cannot be read more accurately. Data for the cul-de-sac area are not available. High water at Nassau, New Providence Island, occurs about 16 minutes after lunar transit of the Greenwich Meridian. This high water interval is based upon the epoch of the principal lunar semidiurnal component.

Future Study

Data collected to date indicate that conventional methods of collecting oceanographic information are not suitable for the type studies needed in the TOTO. Initially, the time interval between observations should be not greater than 15 minutes (the approximate period of a transverse oscillation).

Such short period oscillations may not have sufficient amplitude to significantly affect sound propagation. Should this prove to be true, then the frequency of sampling will be determined by the shortest period oscillation which contributes significantly to variations in physical properties.

Theoretically, the observations should cover the entire water column for a length of time not less than that dictated by the synodic periods of the significant oscillations. For example, the data indicate that a relatively long period oscillation, 100 to 120 hours, causes slow but very significant changes in temperature. The synodic period for a 120-hour component and 24-hour component would be some multiple of 30 hours.

The more synodic periods included in the data record, the more complete the separation will be. A record of 35 days would include 28 synodic periods of the diurnal and 120-hour components as well as 7 complete cycles of the 120-hour period component.

It should be noted that all time variations in physical properties, even though they are periodic, are not manifestations of internal waves. If, for example, stationary fronts (discontinuity layers of oceanographic properties) exist at depths within a body of water, then variations similar to those observed in the TOTO could occur if periodic disturbances of dynamic equilibrium occur. Periodic variations in the slope of isosteric surfaces (such as the Isothermal and Isohaline surfaces) of the discontinuity layer are manifestations of periodic variations in the speed of a permanent current. According to Defant (1952) oscillations of 20 meters or greater of the boundary layer may occur, if, for example, alternating tidal currents of normal strength are present. However, if data are collected as briefly

outlined, and accompanied by auxiliary measurements, then the desired analyses may be made.

The foregoing discussion is intended to emphasize the magnitude of the oceanographic problems in the TOTO and some consideration for data collection. The immense amount of data which must be collected precludes any manual manipulations. Data processing techniques will be discussed in a subsequent report. More formal results of data collected in the TOTO by the Oceanographic Office and other agencies will also be made available.

Bibliography

Defant, Albert

On Internal Waves, Especially those of Tidal periods, Deutsche Hydrographische Zeitschrift; Band 5, Heft 5/6, PP. 231-245, 1952.

Defant, Albert

Physical Oceanography, Vol I and II, 1961.

Fjeldstad, J.

Interne Wellen, Geofys. Publ. 10, No. 8 (Norske Vid. Akad., Oslo), 1935.

Hesselberg, Th. and Sverdrup, H. V.

Die Stabilitätsverhältnisse Des Seewassers Bei Vertikalen Verschiebungen Trans-148, Bergens Musem AARBUK, 1914-15, No. 15, PP. 1-16, Bergen 1915.

Magnitsky, A. W. and French, H. V.

H. O. TR-94, ASWEP Report No. 3, Tongue of the Ocean Research Experiment, 1960.

The Marine Laboratory, University of Miami, Oceanographic Survey of the Tongue of the Ocean; Technical Report, Vol I, 26 Sept 1958.

U. S. Coast and Geodetic Survey

Manual of Harmonic Analysis and Prediction of Tides, Special Publication #98, 1940.